Title

Simulating environmentally-sensitive tree recruitment in vegetation demographic models

Journal

New Phytologist, 235(1)

ISSN

0028-646X

Authors

Hanbury-Brown, Adam R

Powell, Thomas L

Muller-Landau, Helene C

et al.

Publication Date

2022-07-01

DOI

10.1111/nph.18059

Simulating environmentally sensitive tree recruitment in vegetation demographic models

Adam R. Hanbury-Brown[1], Thomas L. Powell[2,3], Helene C. Muller-Landau[4] , S. Joseph Wright[4], Lara M. Kueppers[1,2]
[1]The Energy and Resources Group, 345 Giannini Hall, University of California, Berkeley, CA 94720, USA
[2]Lawrence Berkeley National Laboratory, 1 Cyclotron Rd, Berkeley, CA 94720, USA
[3]Department of Earth and Environmental Systems, The University of the South, 735 University Ave, Sewanee, TN 37383, USA
[4]Smithsonian Tropical Research Institute, Apartado 0843–03092, Balboa, Republic of Panama

ORCIDs
Adam R. Hanbury-Brown: 0000-0003-3751-6257
Tomas L. Powell: 0000-0002-3516-7164
Helene C. Muller-Landau: 0000-0002-3526-9021
S. Joseph Wright: 0000-0003-4260-5676
Lara M. Kueppers: 0000-0002-8134-3579

Author for correspondence:
Adam Hanbury-Brown
Email: ahanburybrown@gmail.com

Received:
Accepted: 9 February 2022

Total word count (excluding summary, references and legends):	6,978	No. of figures	8 (1-7 in color)
Summary:	162	No. tables	1
Introduction:	925	No. of Supporting Information files	10
Materials and Methods:	2,740		
Results:	804		
Discussion:	2371		
Conclusion:	138		

SUMMARY

- Vegetation demographic models (VDMs) endeavor to predict how global forests will respond to climate change. This requires simulating which trees, if any, are able to recruit under changing environmental conditions. We present a new recruitment scheme for VDMs in which functional-type-specific recruitment rates are sensitive to light, soil moisture, and the productivity of reproductive trees.

- We evaluate the scheme by predicting tree recruitment for four tropical tree functional types under varying meteorology and canopy structure at Barro Colorado Island, Panama. We compare predictions to those of a current VDM, quantitative observations, and ecological expectations.
- We find that the scheme improves the magnitude and rank order of recruitment rates among functional types and captures recruitment limitations in response to variable understory light, soil moisture, and changing precipitation regimes.
- Our results indicate that adopting this framework will improve VDM capacity to predict functional-type-specific tree recruitment in response to climate change, thereby improving predictions of future forest distribution, composition, and function.

Key words: forest regeneration, tree recruitment, vegetation demographic models, Earth system models, vegetation dynamics.

INTRODUCTION

Tree recruitment, the rate at which trees grow into the smallest size class tracked by observations, affects global terrestrial ecosystem functioning by determining the rate of regrowth and the future vegetation composition after disturbance (Chazdon, 2003; Johnstone *et al.*, 2016; Martínez-Vilalta & Lloret, 2016). It is the outcome of a dynamic set of environmentally sensitive processes including seed production, dispersal, and seedling establishment (Hubbell *et al.*, 1999; Chazdon, 2003; Wright & Calderón, 2006; Wright *et al.*, 2007; Jabot *et al.*, 2008; Markl *et al.*, 2012; Hacket-Pain *et al.*, 2018). Changing climate and disturbance regimes affect recruitment through their influence on the regeneration niche: the set of environmental conditions needed for plants to produce viable seed, establish as seedlings, and recruit (Grubb, 1977). When an established population's regeneration niche contracts, it results in a change in forest composition or distribution (Engelbrecht *et al.*, 2007; Poorter, 2007; Jabot *et al.*, 2008; Bond, 2008; Valdez *et al.*, 2019). Multiple lines of evidence indicate that climate change and land use are already affecting forest regeneration globally (Chazdon, 2003; Kueppers *et al.*, 2017; Serra-Diaz *et al.*, 2018; Valdez *et al.*, 2019; Sansevero *et al.*, 2020). For example, more severe droughts are linked to declines in post-fire tree recruitment (Stevens-Rumann *et al.*, 2017; Tepley *et al.*, 2017), and increasing hurricane intensity is predicted to change forest composition through differential seedling survival (Comita *et al.*, 2009). Limitations to tree recruitment that change biome boundaries (e.g., Bond, 2008, Sansevero *et al.*, 2020) or the functional composition of a forest (e.g., Johnstone *et al.*, 2006) affect ecosystem resilience and function through structural and physiological traits (Poulter *et al.*, 2011; Zhang *et al.*, 2018; Bonan, 2019), making their prediction essential for forecasting terrestrial biosphere function in the Earth system.

There is growing interest in using vegetation demographic models (VDMs) to represent vegetation dynamics within Earth System Models (ESMs; Bonan, 2015; Fisher *et al.*, 2018). VDMs are "a special class of DGVM, which include representation/tracking of multiple size-classes or individuals of the same PFT, which can encounter multiple light environments within a single climatic grid cell" (Fisher *et al.*, 2018). In contrast to the sophisticated algorithms VDMs use to predict growth and mortality, their representations of recruitment lack a sufficiently process-based approach (McDowell *et al.*, 2020; Hanbury-Brown *et al.*, 2022). Gap models, forest landscape models and mechanistic species distribution models have successfully represented key regeneration processes influencing recruitment such as seed production, dispersal, germination, and seed decay in stand- and landscape-scale simulations (Mladenoff, 2004; Lischke *et al.*, 2006; Lischke & Loffler, 2006; Scheller *et al.*, 2007; Holm *et al.*, 2012; Mok *et al.*, 2012; Larocque *et al.*, 2016), but their modeling approaches are generally less suitable for large scale ESM-coupled simulations because they are computationally expensive and do not conserve carbon. To operate within these constraints many VDMs represent "cohorts" of trees, which belong to the same PFT and size class, and are tracked as pools of carbon occupying spatially implicit forest patches (e.g. Medvigy *et al.*, 2009; Fisher *et al.*, 2015). Each cohort's associated number density of stems is calculated based on representative tree diameter and allometry.

VDMs such as LPJ-GUESS and SEIB-DGVM rely on parameter tuning and rough proxies for understory light and space to calculate recruitment rates and use bioclimatic envelopes to predict PFT distributions (Smith *et al.*, 2001; Sato *et al.*, 2007; Sato, 2009). Bioclimatic envelopes rely on the tenuous assumption that historical correlations between species distributions and climate metrics are sufficient to predict future distributions under novel climates and species assemblages (Pearson & Dawson, 2003; Journé *et al.*, 2020). VDMs based on the Ecosystem Demography (ED) concept (Moorcroft *et al.*, 2001), have dropped bioclimatic envelopes in favor of allowing biogeography to emerge from ecophysiology and competition, but no mechanistic constraints have replaced bioclimatic envelopes for limiting recruitment. Instead, a fixed fraction of net positive carbon production is allocated to a reproductive carbon pool from which new individuals emerge at a rate that is a constant fraction of this pool (Moorcroft *et al.*, 2001; Medvigy *et al.*, 2009; Fisher *et al.*, 2018). This captures the effect of adult productivity on seed production, but environmental conditions in the seedling layer do not affect recruitment in these models. This limits their ability to capture how climate change will affect the regeneration niche, future recruitment limitations, forest distribution, and functional composition. The need to improve predictions is particularly critical for tropical forests which make up the "least certain major component of the global carbon budget" (Mitchard, 2018).

Here we present a new Tree Recruitment Scheme (TRS) for VDMs that more mechanistically constrains recruitment rates based on carbon production from reproductively mature trees, light at the forest floor, and soil moisture in the simulated rooting zone of seedlings. We seek to capture the size dependence of reproductive output and the light- and moisture-dependence of seedling emergence, survival, and the transition out of the seedling pool. By incorporating these environmentally sensitive processes we hope to capture more realistic recruitment responses to varying light, soil moisture, and changing precipitation patterns. We evaluate the TRS by simulating tree recruitment in a seasonally dry tropical forest under observed meteorological conditions, a synthetic El Niño (Powell *et al.*, 2017), wetter-than-observed, and drier-than-observed precipitation scenarios. We compare the scheme's predictions of recruitment rates (at the 1 cm dbh size class) to predictions from the Ecosystem Demography model version 2 (Medvigy *et al.*, 2009), forest demographic data, and ecological expectations and conclude by discussing how the TRS is positioned to improve VDM predictions of forest distribution, composition, and function under global change.

MATERIALS AND METHODS

Model description

VDMs represent the forested landscape as a mosaic of spatially implicit patches varying in time since the last disturbance. This creates a patchwork of heterogenous biotic and abiotic conditions under which cohorts of trees recruit, grow, compete, and die (Fisher *et al.*, 2018). Trees within cohorts are all the same size and PFT, but each patch can contain multiple cohorts of different sizes and PFTs. We designed the TRS, currently implemented in *R* (R Core Team, 2020), to operate within each of these forest patches where it predicts PFT-specific, environmentally sensitive tree recruitment rates. It was developed primarily from studies at BCI, with an initial focus on tropical tree PFTs that vary along axes of drought and shade tolerance (Fig. 2), but is designed to be extensible to all tropical forests. Our primary goal is to mechanistically constrain recruitment. In each daily timestep the TRS receives cohort-level carbon for growth and reproduction (C_{g+r}; net after tissue turnover and allocation to storage) from its host VDM. Regeneration processes, described in detail below, move dynamic fractions of C_{g+r} through a seedbank and seedling pool (Fig. 1) which are tracked in units of carbon. Carbon emerging out of the seedling pool each day is passed back to the VDM and can be converted into a number density of new recruits. Carbon in seeds or seedlings that die or that is allocated to non-seed reproductive biomass, moves to a reproductive litter pool (also passed back to the VDM), thereby conserving carbon.

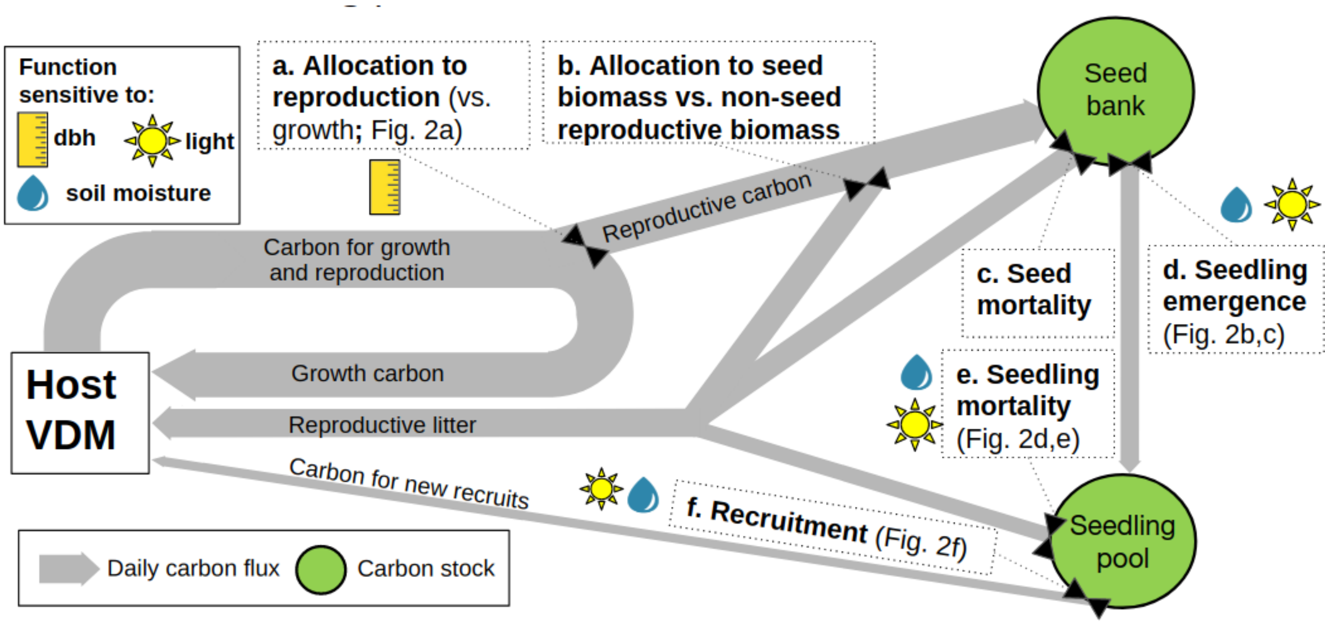

Figure 1. The TRS receives carbon for growth and reproduction from the host VDM. Daily regeneration processes (depicted with hour glasses) transfer reproductive carbon through seed bank and seedling carbon pools (depicted as circles). Processes are sensitive to diameter at breast height (DBH) or environmental conditions (see inset key). The host model's reproductive litter pool receives non-seed reproductive carbon, dead seeds, and dead seedlings. Carbon for new recruits can be passed back to the host VDM in units of carbon or as a number density of new recruits. Parenthetical references to Figure 2 show relationships between regeneration processes and DBH and environmental conditions.

Allocation to reproduction

The probability a tree is reproductive increases sigmoidally with size within species (Visser *et al.*, 2016). Past models assume reproductive allocation is insensitive to size (Smith *et al.*, 2001) or invariant above a fixed size threshold (Sato *et al.*, 2007; Medvigy *et al.*, 2009; Fisher *et al.*, 2015). In contrast, the TRS allocates a dynamic fraction of cohort-level C_{g+r} to reproduction based on the cohort's size and reproductive allocation (RA) function (Eqn 1, Fig. 1a, Fig. 2a). Each mature cohort in the host VDM can contribute to recruitment via the TRS if they are in positive carbon balance. The effective fraction of cohort-level C_{g+r} allocated to reproduction, $F_{E,repro}$ (Eqn 2), is calculated based on a sigmoidal relationship relating the cohort's current dbh to the probability of being reproductive (P_{repro}; Eqn 1). We assume that all reproductive individuals allocate to reproduction at a constant, PFT-specific rate, F_{repro} (see Table 1 for all TRS parameters), which is modified by P_{repro} to calculate $F_{E,repro}$ (Eqn 2)

$$P_{repro} = \frac{e^{(a_{RA}(dbh)+b_{RA})}}{1 + e^{(a_{RA}(dbh)+b_{RA})}} \qquad \text{(Eqn 1)}$$

$$F_{E,repro} = (P_{repro})(F_{repro}) \qquad \text{(Eqn 2)}$$

where a_{RA} and b_{RA} are PFT-specific parameters describing the shape of the sigmoidal curve (Fig. 2a). This functional form is consistent with empirical data (Visser *et al.*, 2016; Minor & Kobe, 2019; Andrus *et al.*, 2020). The TRS subsequently multiplies $F_{E,repro}$ by C_{g+r} to get reproductive carbon per cohort.

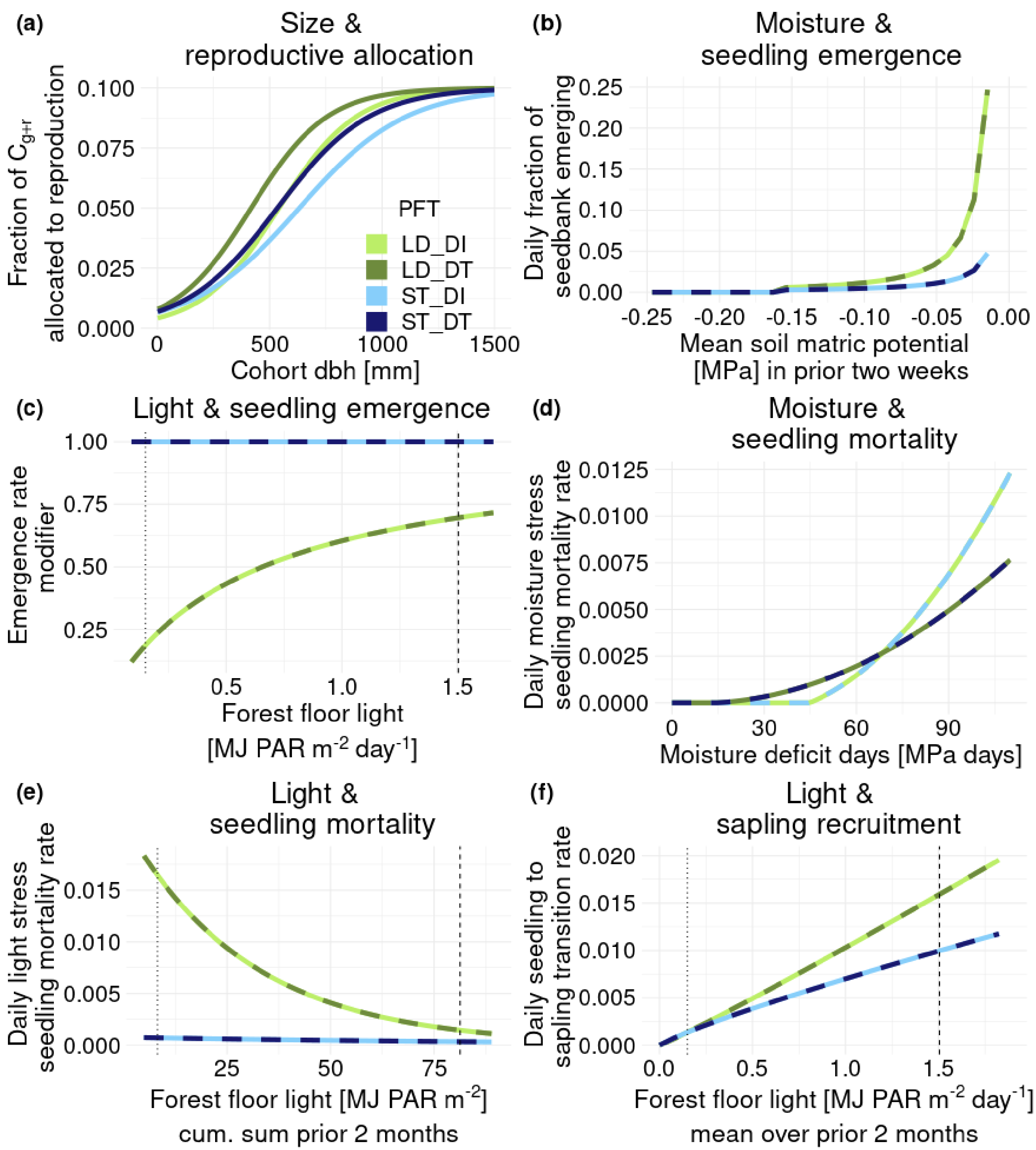

Figure 2. Regeneration processes represented by the Tree Recruitment Scheme are sensitive to size (a), soil moisture (b,d), and light (c,e,f,). Functions are parameterized for four tropical tree PFTs at Barro Colorado Island, Panama: light demanding, drought intolerant (LD-DI); light demanding, drought tolerant (LD-DT); shade tolerant, drought intolerant (ST-DI); and shade tolerant, drought tolerant (ST-

DT). Note that moisture deficit days (panel d) are not equivalent between DT and DI PFTs because they accumulate according to PFT-specific values of Ψ_{crit}. In panels c, e, and f, the dotted vertical lines indicate mean understory light conditions on BCI (2% top of canopy radiation) and the dashed vertical lines indicate conditions in a small-medium sized light gap (20% top of canopy radiation). C_{g+r} = carbon for growth and reproduction; dbh = diameter at breast height; PAR = photosynthetically active radiation.

Allocation to seed vs. non-seed reproductive biomass and seed mortality

In nature, only a subset of the carbon allocated to reproduction becomes seeds, with the rest going to flowers, fruit flesh, capsules, etc. (Wenk *et al.*, 2017), but previous models assume that all reproductive carbon becomes seed (Fisher *et al.*, 2015). The TRS partitions each cohort's reproductive carbon into seed carbon and non-seed reproductive carbon (e.g., flowers, fruit flesh, and capsules) based on a prescribed, PFT-specific fraction of reproductive carbon that is seed, F_{seed} (Fig. 1b). Available seed carbon moves to a seed bank each day and non-seed reproductive carbon moves to a reproductive litter pool (Fig. 1b). Seeds in the seed bank die at a PFT-specific, constant rate, S_{mort}, which represents all modes of seed mortality including predation and decay.

Seedling emergence

Seedling emergence is sensitive to soil moisture (Garwood, 1983; Atondo-Bueno *et al.*, 2016; Ruiz Talonia *et al.*, 2017; Foster *et al.*, 2020) and light (Pearson *et al.*, 2002), but prior regeneration schemes in VDMs either do not represent seedling emergence (Sato *et al.*, 2007; Medvigy *et al.*, 2009) or represent it as an environmentally insensitive constant (Fisher *et al.*, 2015). In the TRS, by contrast, emergence depends on both soil moisture and light.

Light-dependence of germination is captured on day i in a Michaelis-Menten rate modifier [0,1]

$$f(PAR_i) = \frac{PAR_i}{PAR_i + PAR_{crit}} \qquad \text{(Eqn 3)}$$

dependent on PAR_i, the photosynthetically active radiation at the seedling layer on day i, and PAR_{crit}, a PFT-specific threshold governing the shape of the germination response to light (Fig. 2c). Most tropical pioneer species exhibit an increase in germination probability with light, whereas shade-tolerants are insensitive to light (captured by $PAR_{crit} = 0$).

If soil moisture is above a critical threshold, Ψ_{emerg}, the seedling emergence rate on day i, $F_{emerg,i}$, is dynamically calculated based on the mean soil matric potential (SMP) in the top 0-10 cm over a rolling window of days, W_{emerg}, prior to i (Fig. 1d, Fig. 2b). The moisture response parameter, b_{emerg}, modifies the mean seedling emergence coefficient (a_{emerg}) in response to variation in SMP such that

$$F_{emerg,i} = \begin{cases} 0 & SMP_i < \psi_{emerg} \\ f(PAR_i)(a_{emerg})\left(\frac{\sum_{j=i-W_{emerg}}^{i}(1/-SMP_j)}{W_{emerg}}\right)^{b_{emerg}} & SMP_i \geq \psi_{emerg} \end{cases}. \quad \text{(Eqn 4)}$$

Eqn 4 produces pulses of seedling emergence in response to seasonal and interannual precipitation events, and stalls seedling emergence under relatively dry conditions.

This formulation captures observed patterns of variation in seedling emergence in relation to fluctuations in soil moisture (Garwood, 1983; Foster *et al.*, 2020) and spatial variation in understory light levels (Vazquez-Yanes *et al.*, 1990; Pearson *et al.*, 2002). At BCI there is a pulse of seedling emergence at the onset of the wet season with the earliest emerging species responding within ~2 weeks of wet season precipitation (Garwood, 1983). The observed seasonal recruitment pulse at BCI is more pronounced for light demanding (LD, "pioneer") species than for shade tolerant (ST) species (see Fig. 7 in Garwood, 1983), which is represented with a higher value for b_{emerg}.

Moisture and light-sensitive seedling survival

Seedling survival decreases at low soil moisture and low light, affecting forest composition across environmental gradients (Kobe, 1999; Engelbrecht *et al.*, 2007), but this dynamic is missing in previous models. The TRS seeks to capture this with a PFT-specific moisture stress threshold, Ψ_{crit}, below which the seedling pool starts to accumulate moisture deficit days (MDD) similar to the concept of growing degree days. The MDD value on day i is summed within a rolling window of days, W_Ψ, prior to i such that

$$MDD_i = \sum_{j=i-W_\psi}^{i} \begin{cases} 0 & \psi_j \geq \psi_{crit} \\ |\psi_j| - |\psi_{crit}| & \psi_j < \psi_{crit} \end{cases}. \qquad \text{(Eqn 5)}$$

This formulation simultaneously captures the magnitude and duration of moisture stress. We used observations of seedling wilting points from a prior manipulative drought experiment (Engelbrecht & Kursar, 2003; Engelbrecht *et al.*, 2007) to explore the relationship between moisture deficit day accumulation and mortality. We found that observed drought-induced mortality was 0 up to a critical accumulation of MDD, MDD_{crit}, at which point a convex quadratic relationship best explained drought-induced seedling mortality as a function of MDD (Fig. 1e, Fig. 2d, see SI Methods S1 and Fig. S1 for more details). The mortality rate from moisture stress (M_Ψ) on day i is therefore

$$M_{\psi,i} = \begin{cases} 0 & MDD_i < MDD_{crit} \\ a_\psi MDD_i^2 + b_\psi MDD_i + c_\psi & MDD_i \geq MDD_{crit} \end{cases}. \qquad \text{(Eqn 6)}$$

Seedlings also die from insufficient light, which we refer to as light stress. The light stress mortality rate, M_L, on day i is a function of PAR at the seedling layer, $L_{seedling}$, accumulating within a rolling window of days, W_L, prior to i (Fig. 1e, Fig. 2e). Two PFT-specific parameters determine the shape of the negative exponential relationship

$$M_{L,i} = e^{a_{ML}\left(\sum_{j=i-W_L}^{i} L_{seedling,j}\right)+b_{ML}} \qquad \text{(Eqn 7)}$$

where a_{ML} is a PFT-specific light response parameter and b_{ML} is the intercept. We based this function on an analysis by Kobe (1999) who tested four functional forms and found that the negative exponential best described light stress mortality for two shade tolerant (ST) and one light demanding (LD) species that were transplanted into varied light environments. This function is supported by observations that seedling mortality generally increases as light decreases (Kitajima, 1994; Poorter, 1999; Bloor & Grubb, 2003; Comita & Hubbell, 2009). Tolerance to low light conditions varies considerably across species depending on life history strategy (Kitajima, 1994; Wright *et al.*, 2010), which can be captured with PFT-specific values of a_{ML} (Table 1). A background seedling mortality rate, $M_{\text{background}}$, represents other seedling mortality (e.g. herbivory, pathogens, tree fall, etc.). Total seedling mortality is the sum of moisture-dependent, light-dependent and background mortality.

Recruitment

The rate of transition from seedling to sapling increases with understory light (Brokaw, 1985; Rüger *et al.*, 2009), but prior models do not capture this sensitivity (Sato *et al.*, 2007; Fisher *et al.*, 2015) or use proxies for absolute light (Smith *et al.*, 2001). In contrast, recruitment in the TRS is represented with a dynamic seedling to sapling transition rate (TR) which is the fraction of total carbon in the seedling pool, $C_{seedling}$, that recruits each day (Fig. 1f). The TR on day i is calculated as a power function of mean PAR at the seedling layer within a rolling window of days, W_L, prior to i (Fig. 2f). If SMP on day i, Ψ_i, is drier than Ψ_{crit} the transition rate goes to zero such that

$$TR_i = \begin{cases} 0 & \psi_i < \psi_{crit} \\ a_{TR}\left(\frac{\sum_{j=i-W_L}^{i} PAR_j}{W_L}\right)^{b_{TR}} & \psi_i \geq \psi_{crit} \end{cases} \quad \text{(Eqn 8)}$$

where a_{TR} is a coefficient derived from the mean transition rate at observed mean understory PAR (see SI Methods S1) and b_{TR} is the light response modifier. The light response modifier produces accelerating (LD PFTs) or decelerating (ST PFTs) responses to light (Fig. 2f) depending on if b_{TR} is greater or less than 1. Of a variety of functional forms tested at BCI, a power function with species-specific light response modifiers best explained observed variation in recruitment rates under spatially heterogenous patch-level light (Rüger *et al.*, 2009). This formulation is more broadly supported by the growth-mortality functional trade-off axis where LD species can take advantage of higher light conditions through faster relative growth rates (Wright *et al.*, 2010). Carbon transitioning out of the seedling layer can be converted to a number density of new recruits based on the amount of carbon required to form an individual in the smallest size class tracked by the VDM, Z_0, such that the number of new recruits predicted on day i, R_i, is

$$R_i = \frac{(TR_i)(C_{seedling,i})}{Z_0}. \quad \text{(Eqn 9)}$$

Eqn 9 is very similar to how VDMs currently convert reproductive carbon into new recruits, but the key difference is that the TRS only makes this conversion after the functions presented here (Eqns 1–8; Fig. 2) have more mechanistically constrained the amount of carbon available for recruitment.

Simulations at Barro Colorado Island, Panama

We ran the TRS at the 50-ha forest dynamics plot (FDP) on BCI in central Panama (9.151°N, 79.855°W). BCI receives an average of 2662 ± 479 (SD) mm of precipitation per year and experiences a four-month dry season (<100 mm of precipitation per month). All living trees in the FDP > 1 cm in dbh have been censused every 5 years since 1985 (Condit, 1998), which provides the opportunity to benchmark recruitment rates into the 1 cm size class.

We used monthly model output from the Ecosystem Demography model version 2 with hydrodynamics (hereafter referred to as ED2; Medvigy *et al.*, 2009; Powell *et al*., 2018) to run the TRS at BCI. In prior work ED2 was initialized from bare ground at BCI and run with recycled 2008-2014 observed meteorology (i.e. "BASE") until predictions of above ground biomass (AGB) reached dynamic equilibrium after 700 years (see Powell *et al.* (2018), Fig. 3; referred to as simulation year 0 in the simulations presented here). After ED2's spin-up period, its predictions of forest demography were benchmarked against observations of aboveground biomass, size-dependent basal area and tree mortality from the FDP and a series of hydroclimate scenarios were run (discussed below). The TRS requires approximately 4 years of its own spin up before the seed bank and seedling pool come into dynamic equilibrium with mature tree productivity and environmental conditions, so we began TRS evaluations 705 years after ED2 was initialized from bare ground. ED2's output provided the TRS with top of canopy (TOC) solar radiation (W m^{-2}), SMP (we used 6 cm below the surface), and each cohort's dbh and number density. ED2's history of C_{g+r} was not saved, so we used its history of carbon allocated to reproduction, along with knowledge of its relatively simple RA scheme, to back-calculate C_{g+r}. Similar to an offline "one-way-coupled" model setup (Forrest *et al.*, 2020), the TRS's predictions of recruitment were not passed back to ED2.

To test the performance of the TRS, we simulated 15 years of BASE meteorology in a patch with 2% of the TOC light to match average conditions in the understory of the BCI FDP (Rüger *et al.*, 2009), converting solar irradiance to PAR using a conversion rate of 0.45 (García-Rodríguez *et al.*, 2020). We compared predictions of recruitment rates into the 1 cm size from ED2 and the TRS to recruitment from census observations at the BCI FDP between 2005 and 2015 (Condit *et al.*, 2019) because these census intervals overlapped with the observed meteorology used for the ED2 simulations. Following Powell *et al*. (2018), we calculated recruitment only for species that can reach a stature ≥ 20 cm dbh and used expert knowledge (see SI Table S1) to exclude any remaining understory specialists. The FDP census intervals are ~5 years, so we estimated recruitment rates accounting for mortality undetected before individuals' first census following established methods (see Eqn 11 in Kohyama *et al.*, 2018). To compare the TRS's predictions of recruitment to ED2's, we emulated ED2's current recruitment subroutine in *R* which provided more flexibility in making comparisons among scenarios and allowed us to use a value for Z_0 (carbon required to build a new recruit) that matched FDP observations. ED2 allocates a fixed fraction of C_{g+r} to reproduction (F_{repro}; 0.1) and a seedling mortality parameter ($M_{seedling}$; 0.09 day^{-1}) further reduces the carbon available for recruitment.

To evaluate predictions of PFT-specific recruitment across a range of understory light environments, we ran the TRS with 20 years of BASE meteorology in 20 different patches where light at the seedling layer varied between 1 and 100% of TOC solar radiation. To evaluate PFT-specific recruitment responses to variable soil moisture we ran 20-yr simulations in 20 different patches where seasonal patch-level SMP varied from observed soil moisture to unrealistically dry conditions (mean annual SMP ranged from -0.25 to -2.5 MPa), but where light was constant (2% of the TOC), and all patches experienced BASE meteorology. Therefore, soil moisture was decoupled from light conditions in these simulations to demonstrate recruitment responses to soil moisture gradients that may arise from topographic variation within a site.

In addition to BASE meteorology we ran the TRS with ED2 output from three previously published hydroclimate scenarios: 1) a synthetic "El Niño" time series which includes two exceptionally strong droughts, based on observed precipitation during the 1982/83 El Niño at BCI (Powell *et al.*, 2017; Powell *et al*., 2018 Note S2), within 30 years (the "SYN-ENSO" scenario), 2) a "WET" scenario where precipitation increased 30% compared to BASE precipitation, and 3) a "DRY-DS" scenario where dry season (January–April) precipitation was reduced 75% compared to BASE (Powell *et al.*, 2018). For each of these scenarios, we ran the TRS for 30 years and recorded annual PFT-specific recruitment rates. Each precipitation scenario changed soil moisture (Fig. S3) and mature tree productivity (Fig. 3), thereby changing C_{g+r} used by the TRS. ED2 predicts that the ST PFTs have a greater share of AGB than the LD PFTs at BCI (Powell *et al.*, 2018), but the relative share of total forest NPP is more variable among the PFTs over time, and the LD-DT PFT often accounts for the greatest share of NPP (Fig. 3).

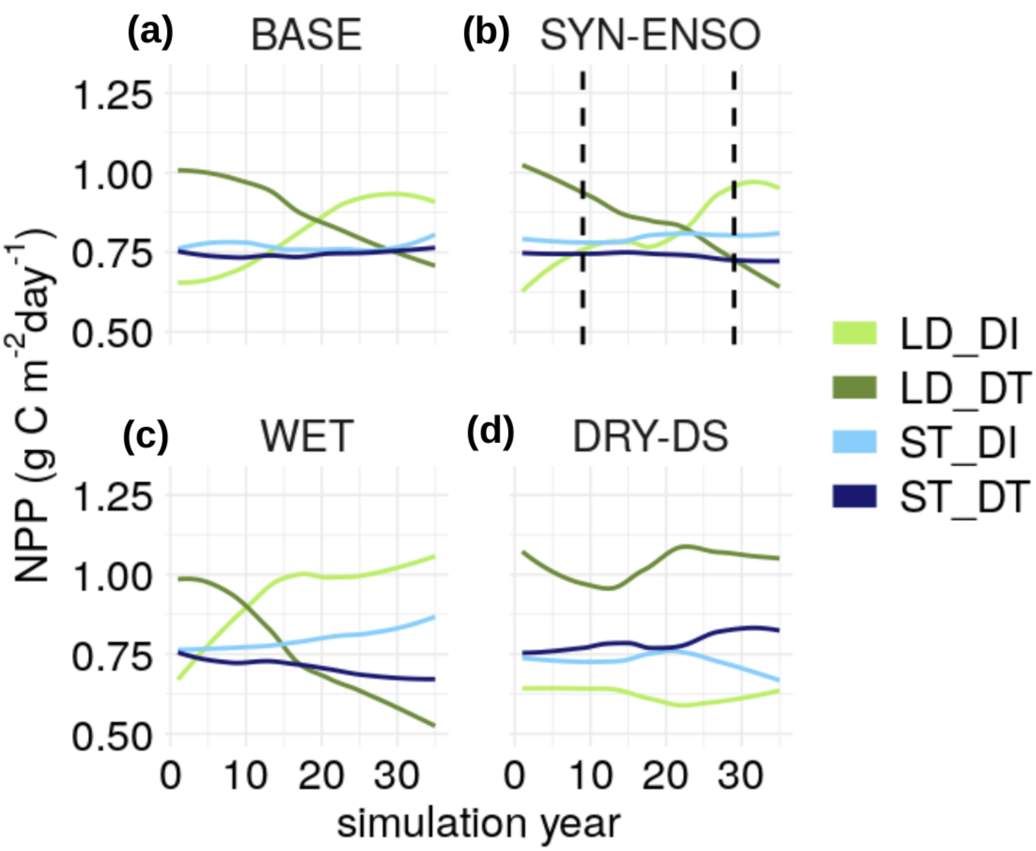

Figure 3. Net primary productivity (NPP) predicted by ED2 under four precipitation scenarios used to run the TRS. BASE = recycled 2008-2014 observed meteorology (a); SYN-ENSO = two exceptionally strong El Niño events within 30 years (b); WET = 30% increase in precipitation compared to BASE (c); DRY-DS = dry season (January–April) precipitation reduced by 75% compared to BASE (d). Dashed lines indicate El Niño events. Note: NPP in the BASE scenario reached dynamic equilibrium (Fig. S4) despite the directional trends apparent over this relatively short 30-yr time period. Lines have a LOESS smoother for easier interpretation of rank order and trends among PFTs. Published estimates of observed PFT-level NPP are not available, but the predicted mean NPP over this period, summed over the four PFTs (2.8 g C m^{-2} day^{-1}), is 15% lower than empirical estimates of total ecosystem-level NPP (3.3 g C m^{-2} day^{-1}; Martínez Cano *et al.*, 2020, Running *et al.*, 2015). LD-DI = light demanding, drought intolerant; LD-DT = light demanding, drought tolerant; ST-DI = shade tolerant, drought intolerant; ST-DI = shade tolerant, drought tolerant.

Parameterization for BCI

We parameterized the TRS with the same four tropical tree PFTs used in Powell *et al.* (2018) which differ along axes of shade tolerance and drought tolerance: 1) light demanding, drought intolerant (LD-DI), 2) light demanding, drought tolerant (LD-DT), 3) shade tolerant, drought intolerant (ST-DI), and 4) shade tolerant, drought tolerant (ST-DT). To calculate PFT-level recruitment benchmarks from species-level observations we used a wood density threshold whereby species above 0.49 g cm^{-3} were assigned to the ST PFT and species below this threshold were assigned to the LD PFT (Powell *et al.* 2018). We categorized species as DT or DI based on three observational datasets including a manipulative drought experiment (Engelbrecht & Kursar, 2003; Engelbrecht *et al.*, 2007) and occurrence probabilities across aridity gradients at the site scale (Harms *et al.*, 2001) and regional scale (Condit *et al.*, 2013; SI Methods S2, Table S2). All parameter values used for these simulations are shown in Table 1. We tested model sensitivity to all parameters by increasing each parameter value by 10% above the default values and evaluating the corresponding change in predicted recruitment rates.

Table 1. Tree Recruitment Scheme default parameterization for Barro Colorado Island (BCI), Panama grouped by regeneration processes shown in Fig. 1; see SI Methods S1 for parameter derivations; PFT = plant functional type; C_{g+r} = carbon for growth and reproduction; RA = reproductive allocation; dbh = diameter at breast height; PAR = photosynthetically active radiation; MDD = Moisture deficit days; LD-DI = light demanding, drought intolerant; LD-DT = light demanding, drought tolerant; ST-DI = shade tolerant, drought intolerant; ST-DI = shade tolerant, drought tolerant.

Name	**Value**	**Units**	**Description**	**Derivation / Source**
		Allocation to reproduction		
F_{repro}	0.1 (all PFTs)	-	Fraction of C_{g+r} allocated to reproduction	Smith *et al.* (2001), Fisher *et al.* (2015) based on Harper (1977)
a_{RA}	LD-DI: 0.0058 LD-DT: 0.0059 ST-DI: 0.0042 ST-DT: 0.0049	Δ RA [Δ dbh]$^{-1}$	Governs RA as function of dbh (logit function coefficient)	Logistic regression fit to observations by Wright *et al.* (2015), Visser *et al.* (2016)
b_{RA}	LD-DI: -3.1380 LD-DT: -2.4607 ST-DI: -2.6518 ST-DT: -2.6171	-	Governs RA as function of dbh (intercept in logit function)	Logistic regression fit to observations by Wright *et al.* (2015), Visser *et al.* (2016)
		Allocation to seed vs. non-seed reproductive biomass and seed mortality		
F_{seed}	0.5 (tuned to 0.24) (all PFTs)	-	Fraction of reproductive C that is seed	Based on range cited by Wenk *et al.* (2017)
S_{mort}	0.0014 (all PFTs)	day^{-1}	Seed mortality rate	Fisher *et al.* (2015) based on Lischke *et al.* (2006)

		Seedling emergence		
a_{emerg}	0.0003	day^{-1}	Coefficient for seedling emergence rate	Calculated from Pearson *et al.* (2002)
b_{emerg}	LD-DI: 1.6 LD-DT: 1.6 ST-DI: 1.2 ST-DT: 1.2	-	Seedling emergence sensitivity to soil moisture	Calibrated to observations of seasonal seedling emergence (Garwood, 1983)
W_{emerg}	14 (all PFTs)	days	Time window for emergence response to soil moisture	Observations of seasonal seedling emergence (Garwood, 1983)
Ψ_{emerg}	-0.15745	MPa	Soil moisture required for emergence	This study, see SI Methods S1
PAR_{crit}	0.656	MJ m^{-2} day^{-1}	Critical PAR level for light-sensitive germination	Based on observations of mean irradiance (PAR) in small gaps ($25m^2$) at BCI (Pearson *et al.*, 2002)
		Moisture and light-sensitive seedling survival		
$M_{background}$	LD-DI: 0.17 LD-DT: 0.18 ST-DI: 0.19 ST-DT: 0.11	yr^{-1}	Background seedling mortality rate	Calculated from seedling censuses done at BCI (2003-2012); Johnson *et al.* (2017)
Ψ_{crit}	DI: -0.176 DT: -0.252	MPa	Seedling moisture stress threshold	Based on observations from Engelbrecht & Kursar (2003), Engelbrecht *et al.* (2005)
MDD_{crit}	DI: 46 DT: 14	-MPa days	Moisture deficit day threshold for seedling mortality	Based on observations from Engelbrecht & Kursar (2003), Engelbrecht *et al.* (2005)
a_{Ψ}	DI: 1.04E-16 DT: 4.07E-17	-	Moisture-based mortality coefficient	Based on observations from Engelbrecht & Kursar (2003), Engelbrecht *et al.* (2005)
b_{Ψ}	DI:-5.5E-10 DT:-6.4E-11	-	Moisture-based mortality coefficient	Based on observations from Engelbrecht & Kursar (2003), Engelbrecht *et al.* (2005)
c_{Ψ}	DI:3.5E-04 DT:1.3E-05	-	Moisture-based mortality coefficient	Based on observations from Engelbrecht & Kursar (2003), Engelbrecht *et al.* (2005)
W_{Ψ}	126 (all PFTs)	days	Rolling window for MDD	Based on observations from Engelbrecht & Kursar (2003), Engelbrecht *et al.* (2005)
a_{ML}	LD:-0.033 ST:-0.00990	-	Light-based mortality coefficient	Based on observations by Kobe (1999)
b_{ML}	LD:-3.84 ST:-7.15	-	Light-based mortality coefficient	Based on observations by Kobe (1999)
W_L	64 (all PFTs)	days	Rolling window for seedling light response	Based on observations by Augspurger (1984)
		Recruitment		
a_{TR}	LD:0.010 ST:0.007	-	Seedling to sapling transition rate coefficient	Derived from parameters used in CLM(ED) and FATES; Fisher *et al.* (2015)
b_{TR}	LD: 1.0653 ST: 0.8615	-	Recruitment light response parameter	Based on Ruger *et al.* (2009)

Convert carbon to number density of recruits				
Z_0	160 (~1 cm dbh; all PFTs)	g C	C per new recruit	Based on value used in ED2 (Powell *et al.* 2018)

RESULTS

Benchmarking recruitment at BCI

Compared to predictions from the default ED2 formulation, the new TRS improves predictions of recruitment magnitude and rank order across all PFTs using default parameters (i.e. no parameter tuning; Fig. 4). ED2 incorrectly predicts that recruitment is dominated by the LD-DT PFT while the TRS correctly predicts that the ST-DT PFT dominates recruitment. Manually adjusting parameters that control the amount of reproductive carbon available for recruitment can further improve biases in the magnitude of recruitment rates for both models compared to their default parameter set. For example, increasing ED2's seedling mortality parameter from 0.09 to 0.986 day^{-1} and reducing F_{seed} in the TRS by half across all PFTs improves predictions of recruitment magnitude in both models (tuned values are used for subsequent results). However, parameter adjustments do not improve ED2 predictions of the rank order of recruitment rates, nor do they address its environmental insensitivity (discussed below). Although the TRS correctly predicts that ST recruitment is greater than LD recruitment it incorrectly predicts that LD-DT recruitment is greater than LD-DI recruitment.

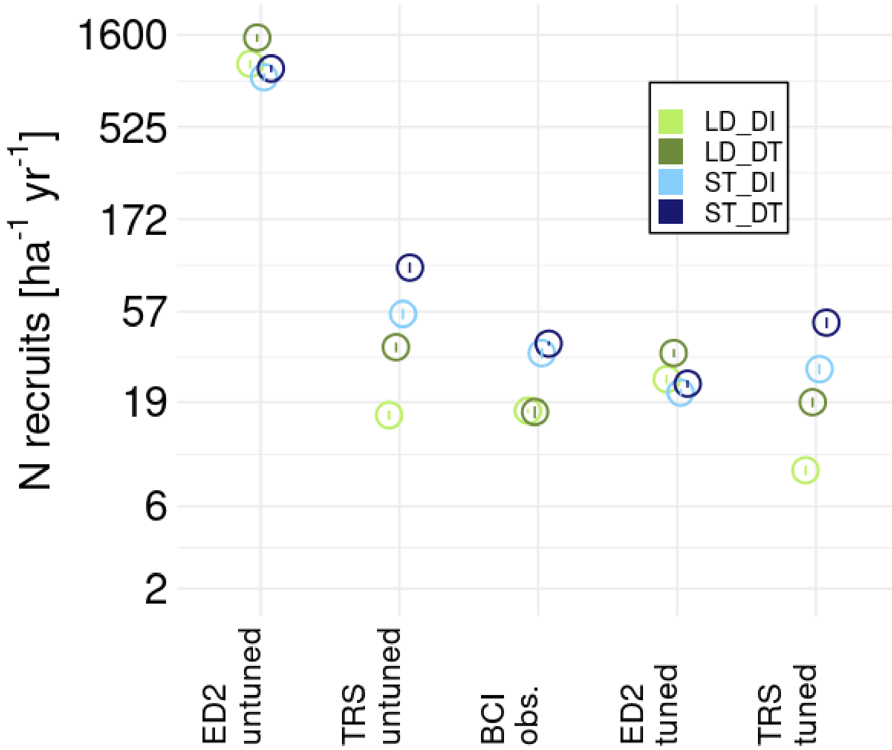

Figure 4. Observed mean annual tree recruitment (at 1-cm dbh) for four plant functional types (PFTs) at BCI (center) compared with model predictions under 20 yr of observed meteorology (2008–2014 recycled) using default and tuned parameter values for the Tree Recruitment Scheme (TRS) and Ecosystem Demography model v.2 with hydrodynamics (ED2). 'TRS tuned' and 'ED2 tuned' are predictions after reducing the TRS's F seed parameter by half and increasing ED2's M seedling parameter from 0.094 to 0.986. 'BCI obs.' are PFT-level mean annual observed recruitment rates averaged from the two 5-yr census intervals between 2005 and 2015 in the BCI Forest Dynamics Plot.

Sensitivity to variable light and soil moisture

Recruitment in ED2 is insensitive to understory light (Fig. 5b). In contrast, the TRS predicts PFT-specific, light-sensitive recruitment responses to varying understory light (Fig. 5a). All PFTs in the TRS show recruitment increasing with light and this variation is strongest for the LD PFTs. Even under high light the LD-DI PFT recruits at a relatively low rate because it comprises a smaller share of total forest NPP under BASE meteorology (Fig. 3a), demonstrating the TRS's dual sensitivity to seedling layer conditions and adult productivity.

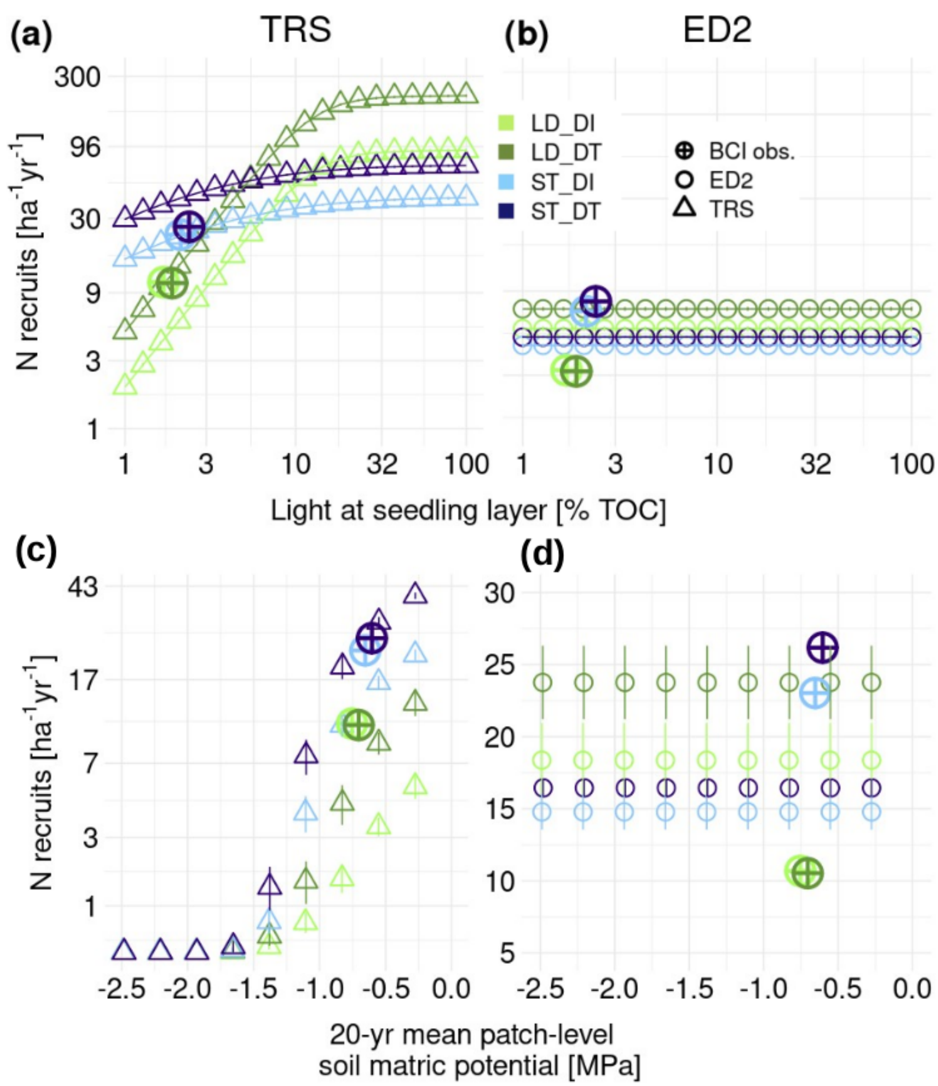

Figure 5. Predictions of tree recruitment (at 1 cm dbh) across a range of idealized patch-level light (a,b) and soil moisture (c,d) conditions with local observed meteorology (2008-2014) at Barro Colorado Island. Observed PFT-specific mean annual recruitment rates ("BCI obs.") are shown for reference and were calculated from 2005–2010 and 2010–2015 census intervals. Observed means are plotted at light levels equal to the mean understory light level across all patches in the Forest Dynamics Plot (Rüger *et al*., 2009) (a,b) and soil moisture equal to the mean measured at the BCI Lutz catchment between 2008 and 2014 (Paton, 2019) (c,d). Error bars show the interannual variation in recruitment within each patch (SD); in many cases these are smaller than the symbol size. TOC = top of canopy.

Among low light patches (2% TOC) that vary in soil moisture (Fig. 5c,d), the TRS predicts PFT-specific, moisture-sensitive recruitment responses (Fig. 5c). All PFTs show complete recruitment failure when the 20-yr mean SMP reaches -2 MPa (Fig. 5c). Recruitment drops faster for the more vulnerable DI PFTs. When soil moisture is high the ST-DI PFT recruits better than the LD-DT PFT despite a much lower share of NPP, reflecting its ability to recruit in low light conditions when moisture is not limiting. However, when SMP drops below -1.0 MPa, soil moisture limits recruitment more than light and all PFTs show minimal recruitment.

Recruitment predictions under ENSO and WET precipitation scenarios

Predictions of recruitment (at 1 cm dbh) responses to ENSO and increasing precipitation (i.e. WET scenario) differ between the TRS and ED2. ED2 and the TRS both show a sharp reduction (~30%) in recruitment for all PFTs across two synthetic El Niño events, but the TRS slightly buffers this reduction for DT PFTs (Fig. 6a,b). A closer look at recruitment dynamics during an El Niño year (Fig. 6c,d) shows that ED2 and the TRS differ in the duration of recruitment failure for DT and DI PFTs. In ED2, drought stress in the adult cohorts causes recruitment to decline in proportion to NPP and then gradually ramp back up as NPP becomes positive at the end of the El Niño event. Recruitment in the TRS only fails when SMP drops below PFT-specific Ψ_{crit} and seedlings persist (but don’t recruit) through the dry season, allowing them to take advantage of wetter conditions with a strong pulse of recruitment at the end of the El Niño dry season (Fig. 6c). This aligns with observations of sapling recovery after the strong 1982/83 El Niño (Condit *et al.*, 2017). The TRS’s environmentally sensitive seedling pool changed the transient recruitment response to El Niño.

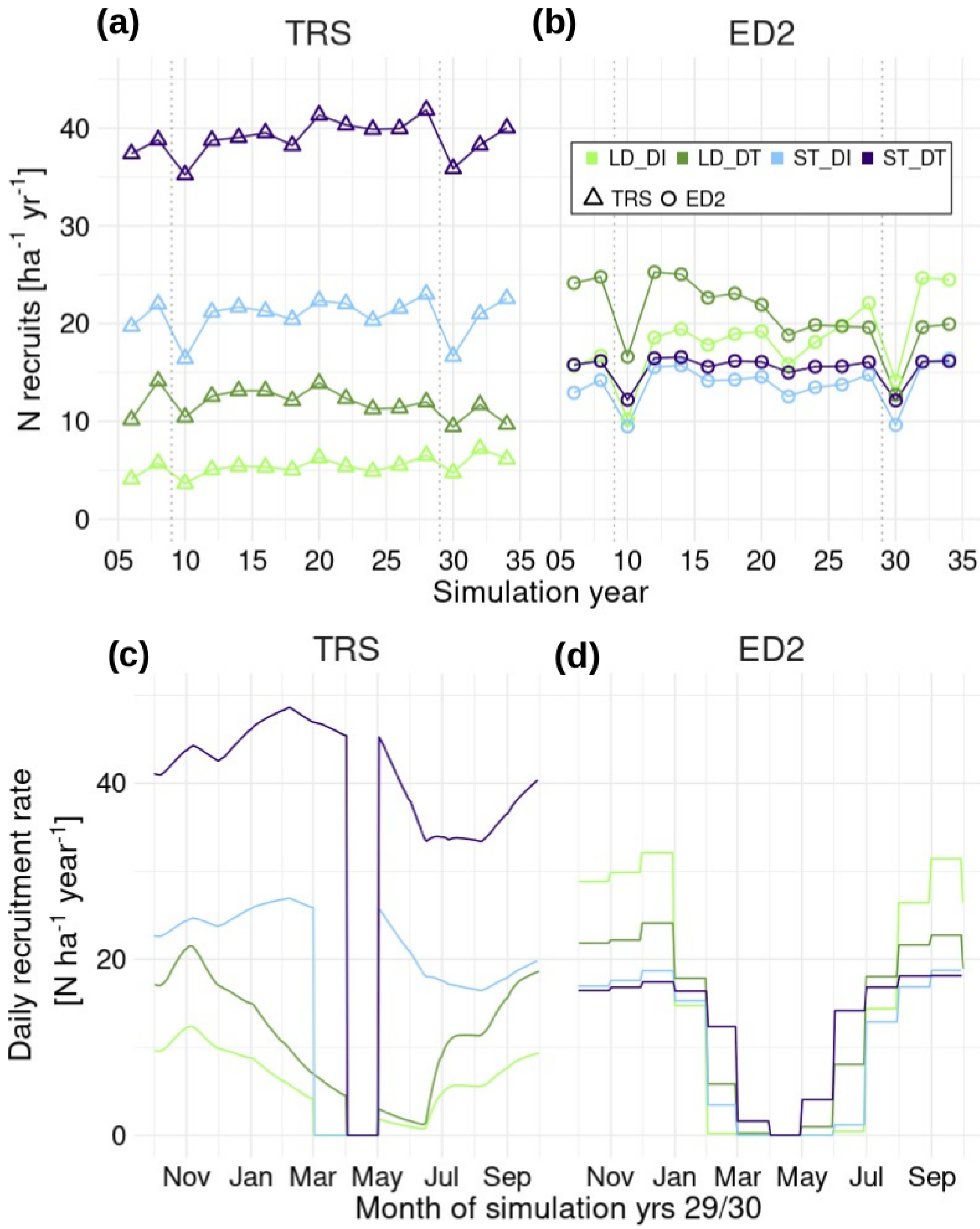

Figure 6. Predictions of tree recruitment (at 1 cm dbh) in a low light patch, 2% top of canopy (TOC)
448 solar radiation, under 30 yrs of local observed meteorology with a strong synthetic El Niño event every 20 years (SYN-ENSO) (a,b). Dotted lines indicate the El Niño years. Seasonal predictions of tree
450 recruitment in a patch with 2% TOC light across the El Niño in simulation years 29/30 are shown in

panels c and d. Note that the ED2 output has a monthly timestep. Soil matric potential is below -2 MPa during March, April, and May (see Fig. S5 for more details).

Under the WET scenario the LD-DI PFT starts to dominate total forest NPP (Fig. 3), which results in different recruitment responses between ED2 and the TRS. ED2 predicts a corresponding, immediate increase in LD-DI recruitment regardless of the light environment (Fig. 7b,d), reflecting its insensitivity to patch-level light. In contrast, the TRS does not allow the LD-DI PFT to dominate recruitment in low light patches (Fig. 7a), because the light component of its regeneration niche is not met despite its increasing share of NPP (Fig. 3). However, under high light the TRS predicts a significant increase in LD-DI recruitment (Fig. 7c), similar to ED2. Under the DRY-DS scenario both models predicted lower recruitment rates, but differ in the timing of recruitment declines (see SI Note 1 and Fig. S2 for more details on the DRY-DS precipitation scenario).

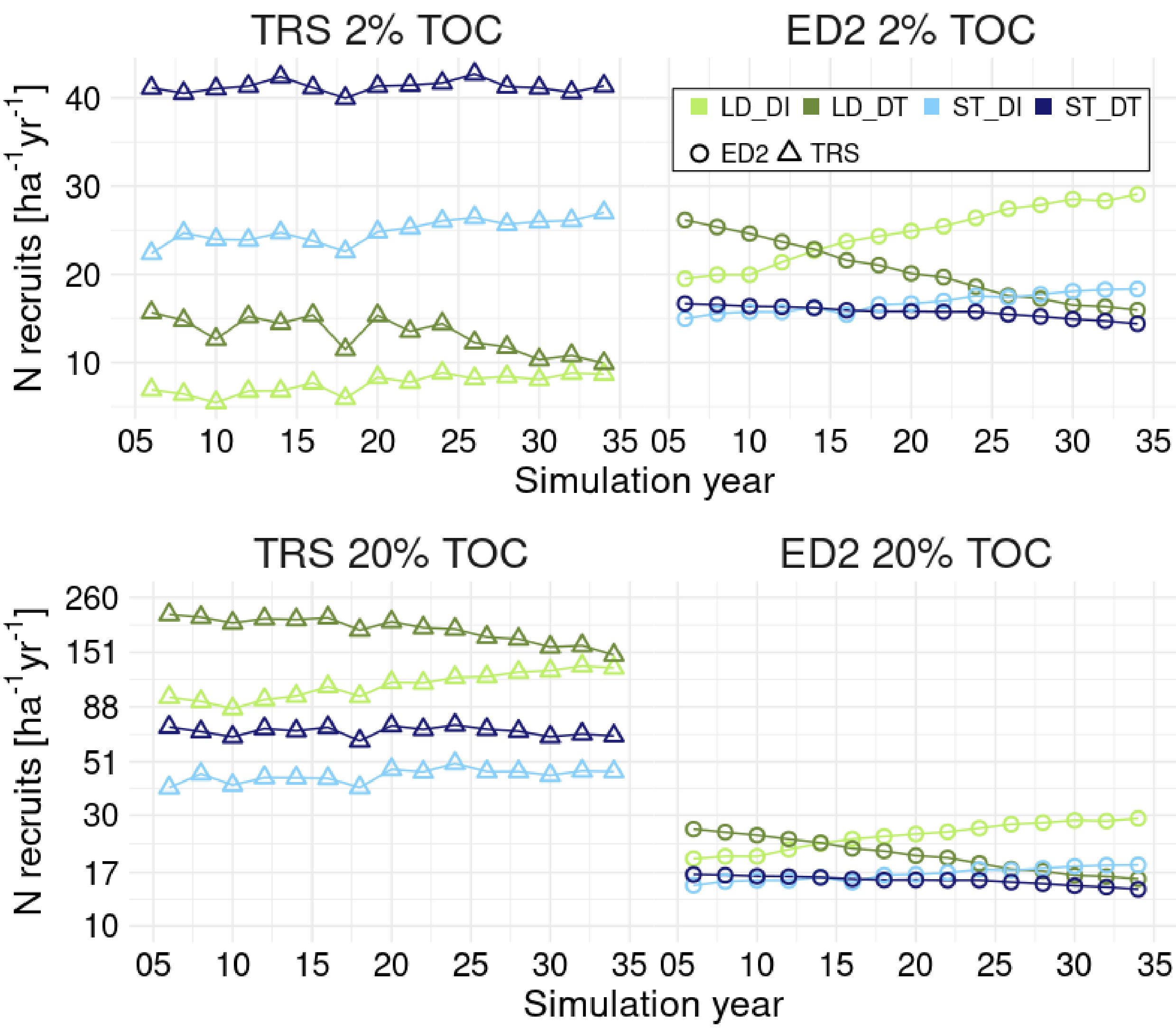

Figure 7. Predictions of tree recruitment (at 1 cm dbh) under 30 yrs of the WET scenario, a 30% increase in precipitation compared to baseline. Predictions are shown under 2% top of canopy (TOC) light (a,b) and 20% TOC light (c,d).

Parameter sensitivity

The light response parameter for seedling mortality (b_{ML}) has the greatest leverage on recruitment outcomes (Fig. 8), which is expected given that light is a key limiting resource in mature tropical forest understories. The remaining top four parameters with the most leverage on recruitment are part of the upstream reproductive allocation scheme (Fig. 8, Table 1). Parameters governing moisture stress mortality, emergence, and transition rates do not show leverage because the parameter sensitivity simulations were run under BASE meteorology where soil moisture does not fall below the observed wilting thresholds (Engelbrecht *et al.*, 2007) required to trigger moisture-based mortality responses.

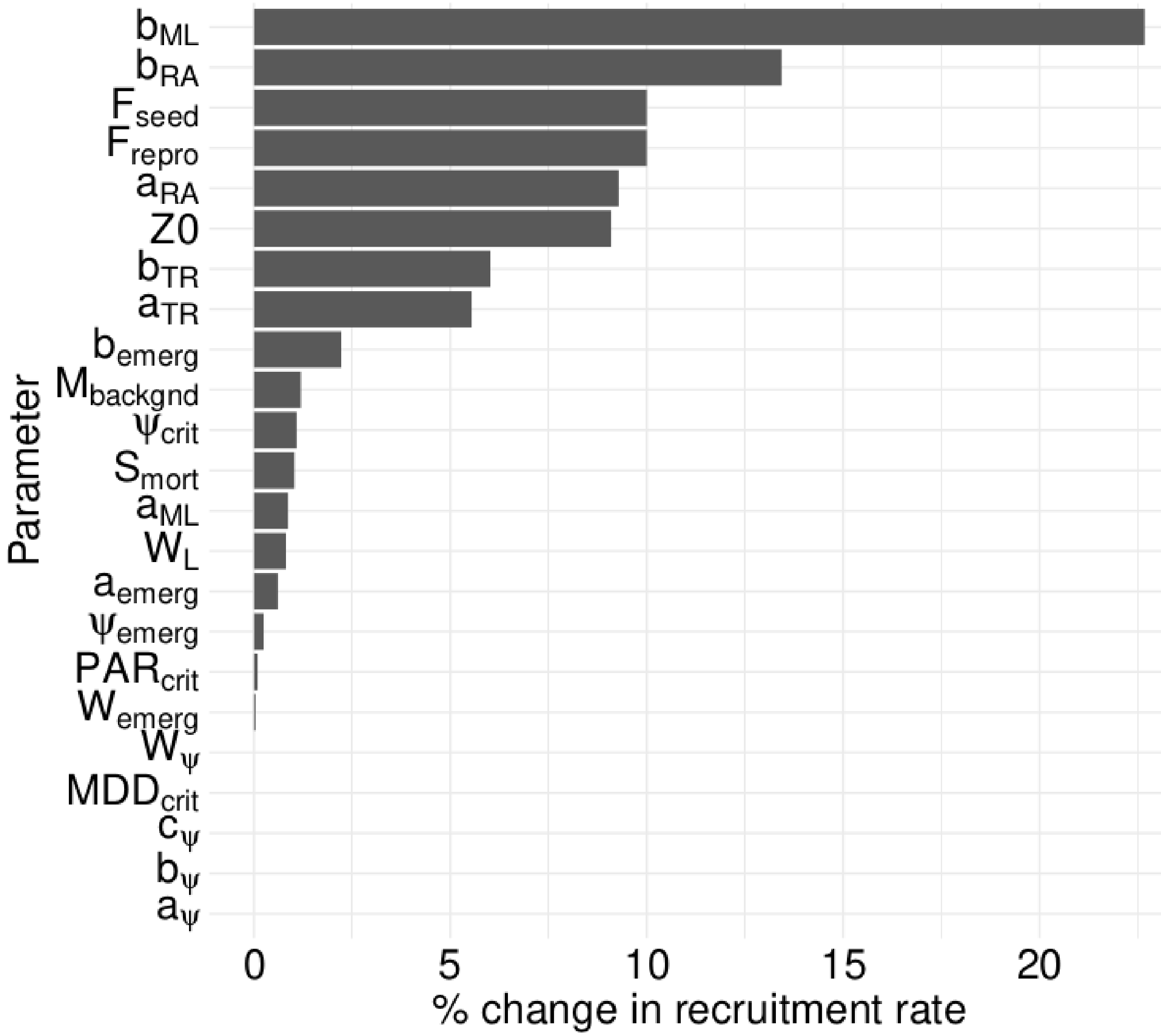

Figure 8. Recruitment sensitivity to a 10% change in parameter value (see Table 1 for parameter descriptions).

DISCUSSION

The TRS predicts tree recruitment as a function of understory light, soil moisture, and productivity of reproductively mature cohorts. We evaluated the TRS by parameterizing it for a seasonally dry tropical forest and running simulations under observed meteorology and canopy structure, variable patch-level understory light and soil moisture, and with three altered precipitation scenarios (ENSO, wetter-than-observed, and drier-than-observed). The TRS improves upon ED2 predictions by capturing recruitment sensitivity to light and soil moisture, and allowing more realistic recruitment responses to environmental heterogeneity without the computational cost of simulating seedling cohorts or individuals explicitly.

Benchmarking recruitment at BCI

We attribute the TRS's improved predictions of recruitment magnitude and PFT rank order (Fig. 4) to PFT-specific, light-sensitive germination, seedling mortality from light stress and light-sensitive seedling to sapling transition rates. Despite its dominant share of total forest NPP, the LD-DT PFT experienced seedling mortality rates almost 13 times greater than the ST PFTs in BCI's understory, resulting in recruitment predictions more consistent with quantitative observations at the BCI FDP (Fig. 4). The TRS's prediction that recruitment is dominated by ST PFTs is consistent with ecological expectations in a mature, closed canopy forest where shade tolerant PFTs should be favored during community assembly (Comita & Hubbell, 2009; Lebrija-Trejos *et al.*, 2010; Wright *et al.*, 2010). In contrast to observations, the TRS predicts that LD-DT recruitment is twice as high as LD-DI (Fig. 4) which could be due to erroneous species assignments to DT and DI PFTs or because we did not simulate observed spatial heterogeneity in patch-level soil moisture at BCI, such as occurs along hillslopes (Becker *et al.*, 1988), or due to soil moisture and NPP biases predicted by ED2.

Sensitivity to variable light and moisture conditions

Light sensitive recruitment in the TRS (Fig. 5) is consistent with prior experimental evidence and ecological expectations showing that LD species recruit at higher densities under brighter conditions, such as in light gaps or forest fragments (Brokaw, 1985; Dupuy & Chazdon, 2008; d'Oliveira & Ribas, 2011). These predictions primarily emerge within the TRS from light-sensitive seedling mortality and seedling-to-sapling transition rates, but the size and productivity of adult cohorts are also influential. For example, the LD-DT PFT is particularly dominant among recruits at high light because of its large share of total forest NPP under BASE meteorology (Fig. 3). PFT-specific responses to increasing light are important for representing gap phase dynamics (Brokaw, 1985) and because disturbance rates are increasing with climate change (Turner, 2010; Seidl *et al.*, 2017), likely chronically increasing understory light. Therefore, incorporating the TRS into VDMs will improve predictions of PFT-specific light responses that mediate functional turnover.

The TRS captured PFT-specific, moisture-sensitive recruitment limitations (Fig. 5), which we attribute to the inclusion of moisture-sensitive seedling emergence, seedling mortality, and seedling to sapling transition rates. The DT PFTs maintained very low recruitment at -2 MPa of SMP due to a more negative (i.e. dry) Ψ_{crit} value, allowing them to accumulate less moisture deficit days than the DI PFTs under dry conditions. Capturing moisture-sensitive recruitment limitations is important for predicting PFT distributions because soil moisture varies dramatically throughout large parts of the tropics and influences differential seedling survival and mature forest composition (Engelbrecht *et al.*, 2007; Condit *et al.*, 2013). By more accurately reflecting the early life-stage at which moisture-based environmental filtering is believed to take place (Engelbrecht *et al.*, 2007), the TRS will enable VDMs to more mechanistically predict functional turnover across topographic and regional moisture gradients and in response to changing precipitation regimes (Martínez-Vilalta & Lloret, 2016).

The TRS's representation of moisture-sensitive recruitment is more consistent with ecological expectations and observations (Engelbrecht *et al.*, 2007) compared to ED2, which assumes that recruitment rates are insensitive to SMP (Fig. 5). Enabling PFT-specific, moisture-sensitive recruitment rates is helpful for VDMs that already have a sophisticated representation of mature plant hydraulics because the understory is typically more humid than the canopy (Fetcher *et al.*, 1985), which can help seedlings survive drought in some contexts (Gómez-Aparicio *et al.*, 2008; Andivia *et al.*, 2018). Conversely, their shallower root systems can leave them more vulnerable to wide fluctuations in soil moisture occurring near the soil surface (Brum *et al.*, 2018). Representing these aspects of the regeneration niche will help VDMs predict forest composition in response to simultaneous but potentially different hydrological conditions experienced by the canopy and the seedling layer.

Responses to ENSO and WET precipitation scenarios

The TRS's more complete representation of the regeneration niche creates novel predictions of how recruitment of 1-cm dbh saplings will respond to varying meteorological scenarios. Unlike ED2, the TRS allowed DT sapling recruitment to continue into March (Fig. 6c) until SMP dropped below the DT Ψ_{crit} value, thereby capturing PFT-specific responses to seedling layer conditions under El Niño. It also captures a large pulse of recruitment from a persisting seedling pool when the El Niño dry season ends (Fig. 6c). The TRS's ability to capture PFT-specific recruitment responses to El Niño is consistent with observations showing that some seedlings persist through severe El Niños (Engelbrecht *et al.*, 2002), some suffer increased mortality (Gilbert *et al.*, 2001), and that recruitment responses vary by PFT (Slik, 2004). The TRS's temporal decoupling of adult productivity from seedling dynamics allows understory light and soil moisture to drive the transient recruitment response instead of remaining directly proportional to adult NPP as occurs in ED2 (Fig. 6d). Decoupling recruitment from adult NPP by including a seed bank and a seedling pool reproduced observed time lags between seed production and seedling recruitment (Garwood, 1983; Wright & Muller-Landau, 2005) as well as time lags between seedling emergence and recruitment into the 1 cm size class (Chang-Yang *et al.*, 2021). However, the residence time of surviving carbon in the seedling pool, 737 days, may still be shorter than the time it takes for many seedlings in closed canopy tropical forests to recruit (Chang-Yang *et al.*, 2021). Many tropical forest trees lose their leaves in response to El Niño (Detto *et al.*, 2018) letting more light into the understory, which is observed to simultaneously increase understory recruitment and mortality rates depending on functional traits such as wood density (Slik, 2004). The TRS is better positioned to predict these PFT-specific recruitment responses to changing understory conditions as El Niño events become more frequent and severe (Haszpra *et al.*, 2020).

Recruitment predictions under the WET scenario demonstrate the TRS's dual sensitivity to changes in adult productivity and seedling layer conditions. As precipitation increases under the WET scenario the LD-DI PFT dominates total forest NPP (Fig. 3), but the TRS only allows this to translate into recruitment dominance under higher light (Fig. 7c). Conversely, under low light, the TRS only allows recruitment to increase slightly in response to increased LD-DI propagule pressure; low light stops it from dominating recruitment (Fig. 7a). This is consistent with theory and observations that recruitment can be limited by both propagule pressure and environmental filtering during establishment (Jabot *et al.*, 2008). The TRS's dual sensitivity to adult productivity and seedling layer conditions also means that it will provide the host VDM with a seedling layer composition more reflective of forest composition and understory conditions in any given timestep. This is significant because when a disturbance occurs, pulses of recruitment arise from the existing seedling layer, thereby influencing the composition of trees recruiting into the canopy (Brokaw, 1985).

Compatibility with VDMs

The TRS is positioned to improve VDMs by making the representation of tree recruitment more mechanistic while maintaining a computationally efficient approach. It tracks pools of carbon instead of individuals or cohorts, regeneration processes are predicted as a function of variables that are already tracked by VDMs, and carbon is conserved. The TRS can be run at any site where a host VDM can run, which at a minimum requires local meteorological data and a PFT parameter set. Predictions of recruitment can be evaluated most readily at long term forest dynamics plots with repeated census events that track all trees down to the 1 cm dbh size class (e.g. the CTFS-ForetsGeo plot network; Davies *et al.*, 2021), but once the TRS is coupled to a host VDM it will be possible to evaluate recruitment into larger size classes. In sum, the TRS's formulation is designed to be compatible with existing VDM model architecture and observational data.

The TRS minimizes the introduction of new, sensitive parameters that are hard to empirically constrain. Four out of the five most sensitive TRS parameters are part of the size dependent reproductive allocation (RA) function (Fig. 8, Eqn 1), which is expected because RA determines the amount of carbon flowing to all subsequent processes (Fig. 1). F_{repro} already exists in VDMs and it is possible to use existing litter fall data to empirically constrain it in tropical forests (Hanbury-Brown *et al.*, 2022). F_{seed} has not been quantified at the ecosystem or PFT level, but is measurable from field observations (Wenk *et al.*, 2017), highlighting the need and opportunity to quantify it at VDM-relevant scales. The probabilistic relationship between size and RA (governed by a_{RA} and b_{RA}) can be derived from logistic regression applied to readily available observations of dbh and reproductive status (e.g. Visser *et al*., 2016). The light response parameter for seedling mortality (b_{ML}) can be derived from observations of seedling mortality under experimentally manipulated light (e.g. Augspurger, 1984; Kobe, 1999; Balderrama & Chazdon, 2005). With the exception of a_{TR} (discussed below), the remaining parameters are observable and have less leverage on recruitment, but would still need to be quantified or synthesized to run the TRS in extra-tropical biomes or with new PFTs.

Limitations and future work

Evaluating the TRS in a one-way coupled configuration (i.e. offline from a host VDM) allowed us to evaluate the TRS's behavior in a reduced complexity environment without idiosyncratic host model feedbacks that are hard to diagnose. However, until the TRS is fully integrated into a VDM we can't assess how feedbacks between recruitment and adult demographics will influence predictions of future forest composition. We avoided simulations longer than 30 years for this reason. Secondly, the TRS only includes the first order processes limiting tree recruitment within tropical forest patches. We did not address dispersal because it is an inter-patch process that should be implemented directly in VDMs in a way that is congruent with how each model abstracts spatial processes. The representation of PFT-specific inter-patch dispersal limitation (which could be based on traits such as seed size) will likely alter the recruitment rates presented here because more dispersal limited PFTs will be less likely to reach new high resource patches. The TRS also does not address vegetative propagation and post-disturbance resprouting, known to be an important regeneration strategy (Dietze & Clark, 2008; Clarke *et al.*, 2013), because this process should be embedded within each VDM’s storage allocation scheme. Despite these limitations, testing and presenting the TRS as an offline module is consistent with recent calls from the Earth system modeling community for “modular complexity as a strategy” whereby new functionality is organized as modules to mitigate the intractability of increasingly complex ESM components (Fisher & Koven, 2020).

Following the need to balance process fidelity with manageable complexity and computational cost (Fisher & Koven, 2020), we focused on a first order set of processes that we hypothesize is required to capture future recruitment limitations in tropical forests under climate change. However, the TRS omits processes that may require additional consideration. Pathogen attack (Spear *et al.*, 2015) and herbivory (Weissflog *et al.*, 2018) are both known to play roles iparameters regulating seedling population dynamics at the species level and susceptibility to these causes of mortality may covary with functional traits (Coley & Barone, 1996; Spear & Broders, 2021). We used a constant seed mortality rate because we lacked the data to parameterize PFT-specific environmentally sensitive seed mortality in tropical forests and the parameter had relatively little leverage on recruitment rates (Fig. 8). Nevertheless, seed mortality rates likely vary among stands, biomes, and PFTs by more than the 10% value used in our parameter sensitivity experiment (Notman & Gorchov, 2001; Obroucheva *et al.*, 2016), indicating the need for further evaluation. Nitrogen availability is believed to influence the functional composition of recruits during secondary forest development (Batterman *et al.*, 2013) indicating that nutrient limitations on recruitment may be important to represent. There is evidence that seed production varies with interannual variation in solar irradiance, precipitation, and stand structure (Wright & Calderón, 2006; O’Brien *et al.*, 2018; Hacket-Pain *et al.*, 2018; Detto *et al.*, 2018; Minor & Kobe, 2019; Andrus *et al.*, 2020) and a representation of these sensitivities may help facilitate the prediction of masting in future models (Vacchiano *et al.*, 2018), but observations of how RA varies with these variables is still missing for most tropical tree PFTs, so we have not included environmentally sensitive RA here. Currently, all seedlings in the TRS access water at the same depth, but seedling rooting depth is a critical functional trait mediating seedling physiological responses to drought (Brum *et al.*, 2018), making this a key area for future data collection, synthesis, and algorithm development. Additionally, manipulative experiments analyzing how vapor pressure deficit and temperature extremes interact with soil moisture (e.g. Will *et al.*, 2013) to affect seedling mortality would improve upon existing drought experiments (e.g. Engelbrecht & Kursar, 2003; Engelbrecht *et al.*, 2007) and may facilitate more robust algorithms for moisture stress mortality.

We did not implement a carbon assimilation scheme for the seedling layer. Instead, following the current ED-based convention (Moorcroft *et al.*, 2001; Fisher *et al.*, 2015) all carbon used to produce new recruits must come from the stock of C_{g+r}. This is done to avoid resolving photosynthesis for many small cohorts of seedlings, but the corresponding loss of process fidelity means that the fraction of seedling carbon that becomes new recruits at mean understory light (calculated using a_{TR}) is not comparable with observations of seedling to sapling (>= 1 cm dbh) transition probabilities. Future work is required to assess the complexity-fidelity tradeoffs associated with implementing a simple carbon assimilation scheme in the seedling pool to allow for easier model-data intercomparison of this transition. Additional functions, such as temperature-sensitive seedling emergence for extra-tropical forests, could easily be added to the TRS, making the framework presented here (Fig. 1) extensible globally.

CONCLUSION

The TRS provides a more mechanistic constraint on the amount of carbon available for recruitment within VDMs, thereby improving predictions of recruitment compared to a current VDM. Representing tree recruitment as the outcome of critical regeneration processes sensitive to carbon production, light, and soil moisture, enabled predictions of recruitment in a tropical forest that are more consistent with prior observations and ecological expectations. The core infrastructure of the scheme is simple and versatile, and the scheme's parameter set is designed to be minimal and observable. Parameter estimation may require additional empirical synthesis and/or new observations to constrain outside of well-studied ecosystems. Through its improved representation of the regeneration niche, the TRS is well positioned to advance predictions of future tree recruitment under changing climate and disturbance regimes. This is essential to predicting future forest composition, distribution, and function.

ACKNOWLEDGMENTS

A. R. Hanbury-Brown, T. L. Powell, and L. M. Kueppers were supported as part of the Next Generation Ecosystem Experiments-Tropics (NGEE-Tropics), funded by the U.S. Department of Energy, Office of Science, Office of Biological and Environmental Research under award number DE-AC02-05CH11231. We used the ForestGEO benchmarking driver, developed by Dan Johnson and Ryan Knox, to calculate forest demographic rates used for benchmarking the simulations. Seedling census data supplied by Liza Comita and Dan Johnson were used to calculate background seedling mortality rates. The BCI tree censuses were made possible by National Science Foundation grants to Stephen P. Hubbell: DEB-0640386, DEB-0425651, DEB-0346488, DEB-0129874, DEB-00753102, DEB-9909347, DEB-9615226, DEB-9615226, DEB-9405933, DEB-9221033, DEB-9100058, DEB-8906869, DEB-8605042, DEB-8206992, DEB-7922197, and by support from the Forest Global Earth Observatory, the Smithsonian Tropical Research Institute, the John D. and Catherine T. MacArthur Foundation, the Mellon Foundation, the Small World Institute Fund, and numerous private individuals, and through the hard work of over 100 people from 10 countries over the past three decades. The plot project is part the Forest Global Earth Observatory (ForestGEO), a global network of large-scale demographic tree plots.

AUTHOR CONTRIBUTIONS

Conceptualization and Investigation A. R. Hanbury-Brown and L. M. Kueppers; Resources and Data Curation, T. L. Powell, H. C. Muller-Landau, S. J. Wright; Writing-Original Draft, A R. Hanbury-Brown; Writing – Review & Editing, A. R. Hanbury-Brown, L. M. Kueppers, T. L. Powell, H. C. Muller-Landau, S. J. Wright; Software, A. R. Hanbury-Brown.

DATA AVAILABILITY

The Barro Colorado Island Tree Reproduction Dataset is openly available through the Smithsonian Tropical Research Institute at https://doi.org/10.5479/si.data.201511251100 (Wright *et al.*, 2015)

The Barro Colorado Island seedling census data is openly available through Dryad at https://datadryad.org/stash/dataset/doi:10.5061/dryad.fm654 (Visser *et al.*, 2016)

The data used to classify species as canopy trees, midstory specialists, and understory specialists is available in SI Table S1.

The Tree Recruitment Scheme source code and model data output is openly available on github at https://github.com/adamhb/regeneration_submodel

The data used to run the Tree Recruitment Scheme is freely available on Zenodo at https://doi.org/10.5281/zenodo.5498285

REFERENCES

Andivia E, Madrigal-González J, Villar-Salvador P, Zavala MA. **2018**. Do adult trees increase conspecific juvenile resilience to recurrent droughts? Implications for forest regeneration. *Ecosphere* **9**: e02282–e02282.

Andrus RA, Harvey BJ, Hoffman A, Veblen TT. **2020**. Reproductive maturity and cone abundance vary with tree size and stand basal area for two widely distributed conifers. *Ecosphere* **11**. 10.1002/ecs2.3092

Anderson-Teixeira KJ, Davies SJ, Bennett AC, Gonzalez-Akre EB, Muller-Landau HC, Joseph Wright S, Abu Salim K, Almeyda Zambrano AM, Alonso A, Baltzer JL, et al. 2015. CTFS-ForestGEO: A worldwide network monitoring forests in an era of global change. *Global Change Biology* **21**: 528–549.

Atondo-Bueno EJ, López-Barrera F, Bonilla-Moheno M, Williams-Linera G, Ramírez-Marcial N. **2016**. Direct seeding of *Oreomunnea mexicana*, a threatened tree species from Southeastern Mexico. *New Forests* **47**: 845–860.

Augspurger CK. **1984**. Light Requirements of Neotropical Tree Seedlings : A Comparative Study of Growth and Survival. *Journal of Ecology* **72**: 777–795.

Balderrama SIV, Chazdon RL. **2005**. Light-dependent seedling survival and growth of four tree species in Costa Rican second-growth rain forests. *Journal of Tropical Ecology* **21**: 383–395.

Batterman SA, Hedin LO, van Breugel M, Ransijn J, Craven DJ, Hall JS. **2013**. Key role of symbiotic dinitrogen fixation in tropical forest secondary succession. *Nature* **502**: 224–227.

Becker P, Rabenold PE, Idol JR, Smith AP. **1988**. Water Potential Gradients for Gaps and Slopes in a Panamanian Tropical Moist Forest's Dry Season. *Journal of Tropical Ecology* **4**: 173–184.

Bloor JMG, Grubb PJ. **2003**. Growth and mortality in high and low light: Trends among 15 shade-tolerant tropical rain forest tree species. *Journal of Ecology* **91**: 77–85.

Bonan G. **2015**. *Ecological Climatology: Concepts and Applications*. Cambridge, UK: Cambridge University Press.

Bonan G. **2019**. *Climate Change and Terrestrial Ecosystem Modeling*. Cambridge, UK: Cambridge University Press.

Bond WJ. **2008**. What Limits Trees in C 4 Grasslands and Savannas? *Annual Review of Ecology, Evolution, and Systematics* **39**: 641–659.

Brokaw NVL. **1985**. Gap-phase regeneration in a tropical forest. *Ecology* **66**: 682–687.

Brum M, Vadeboncoeur MA, Ivanov V, Asbjornsen H, Saleska S, Alves LF, Penha D, Dias JD, Aragão LEOC, Barros F, *et al.* 2019. Hydrological niche segregation defines forest structure and drought tolerance strategies in a seasonal Amazon forest. *Journal of Ecology* **107**: 318–333.

Chang-Yang C-H, Needham J, Lu C-L, Hsieh C-F, Sun I-F, McMahon SM. **2021**. Closing the life cycle of forest trees: The difficult dynamics of seedling-to-sapling transitions in a subtropical rainforest. *Journal of Ecology* **109**: 2705–2716.

Chazdon RL. **2003**. Tropical forest recovery: Legacies of human impact and natural disturbances. *Perspectives in Plant Ecology, Evolution and Systematics* **6**: 51–71.

Clarke PJ, Lawes MJ, Midgley JJ, Lamont BB, Ojeda F, Burrows GE, Enright NJ, Knox KJEE. **2013**. Resprouting as a key functional trait: how buds, protection and resources drive persistence after fire. *New Phytologist* **197**: 19–35.

Coley PD, Barone JA. **1996**. Herbivory and plant defenses in tropical forests. *Annual Review of Ecology and Systematics* **27**: 305–335.

Comita LS, Hubbell SP. **2009**. Local neighborhood and species shade tolerance influence survival in a diverse seedling bank. *Ecology* **90**: 328–334.

Comita LS, Uriarte M, Thompson J, Jonckheere I, Canham CD, Zimmerman JK. **2009**. Abiotic and biotic drivers of seedling survival in a hurricane-impacted tropical forest. *Journal of Ecology* **97**: 1346–1359.

Condit R. **1998**. *Tropical Forest Census Plots*. Springer-Verlag and R. G. Landes Company, Berlin, Germany, and Georgetown, Texas.

Condit R, Engelbrecht BMJ, Pino D, Pérez R, Turner BL. **2013**. Species distributions in response to individual soil nutrients and seasonal drought across a community of tropical trees. *Proceedings of the National Academy of Sciences of the United States of America* **110**: 5064–8.

Condit R, Pérez R, Lao S, Aguilar S, Hubbell SP. **2017**. Demographic trends and climate over 35 years in the Barro Colorado 50 ha plot. *Forest Ecosystems* **4**: 17.

Condit R, Perez R, Aguilar S, Lao S, Foster RB, Hubbell S. **2019**. Complete data from the Barro Colorado 50-ha plot: 423617 trees, 35 years. Dryad, https://doi.org/10.15146/5xcp-0d46.

Davies SJ, Abiem I, Abu Salim K, Aguilar S, Allen D, Alonso A, Anderson-Teixeira K, Andrade A, Arellano G, Ashton PS, *et al.* 2021. ForestGEO: Understanding forest diversity and dynamics through a global observatory network. *Biological Conservation* **253**: 108907.

Detto M, Wright SJ, Calderón O, Muller-Landau HC. **2018**. Resource acquisition and reproductive strategies of tropical forest in response to the El Niño–Southern Oscillation. *Nature Communications* **9**: 913.

Dietze MC, Clark JS. **2008**. Changing the gap dynamics paradigm: Vegetative regeneration control on forest response tO disturbance. *Ecological Monographs* **78**: 331–347.

Dupuy JM, Chazdon RL. **2008**. Interacting effects of canopy gap, understory vegetation and leaf litter on tree seedling recruitment and composition in tropical secondary forests. *Forest Ecology and Management* **255**: 3716–3725.

Engelbrecht BMJ, Comita LS, Condit R, Kursar T, Tyree MT, Turner BL, Hubbell SP. **2007**. Drought sensitivity shapes species distribution patterns in tropical forests. *Nature* **447**: 80–82.

Engelbrecht BMJ, Kursar TA. **2003**. Comparative drought-resistance of seedlings of 28 species of co-occurring tropical woody plants. *Oecologia* **136**: 383–393.

Engelbrecht BMJ, Wright SJ, De Steven D. **2002**. Survival and ecophysiology of tree seedlings during El Niño drought in a tropical moist forest in Panama. *Journal of Tropical Ecology* **18**: 569–579.

Fetcher N, Oberbauer SF, Strain BR. **1985**. Vegetation effects on microclimate in lowland tropical forest in Costa Rica. *International Journal of Biometeorology* **29**: 145–155.

Fisher RA, Christoffersen O, Longo M, Viskari T, Koven CD, Anderegg WRL, Dietze MC, Farrior CE, Holm JA, Hurtt GC, *et al.* 2018. Vegetation demographics in Earth System Models : A review of progress and priorities. *Global Change Biology* **24**: 35–54.

Fisher RA, Koven CD. **2020**. Perspectives on the Future of Land Surface Models and the Challenges of Representing Complex Terrestrial Systems. *Journal of Advances in Modeling Earth Systems* **12**: e2018MS001453.

Fisher RA, Muszala S, Verteinstein M, Lawrence P, Xu C, McDowell NG, Knox RG, Koven C, Holm J, Rogers BM, *et al.* 2015. Taking off the training wheels: The properties of a dynamic vegetation model without climate envelopes, CLM4.5(ED). *Geoscientific Model Development* **8**: 3593–3619.

Forrest M, Tost H, Lelieveld J, Hickler T. **2020**. Including vegetation dynamics in an atmospheric chemistry-enabled general circulation model: Linking LPJ-GUESS (v4.0) with the EMAC modelling system (v2.53). *Geoscientific Model Development* **13**: 1285–1309.

Foster AC, Martin PH, Redmond MD. **2020**. Soil moisture strongly limits Douglas-fir seedling establishment near its upper elevational limit in the southern Rocky Mountains. *Canadian Journal of Forest Research* **50**: 837–842.

García-Rodríguez A, García-Rodríguez S, Díez-Mediavilla M, Alonso-Tristán C. **2020**. Photosynthetic Active Radiation, Solar Irradiance and the CIE Standard Sky Classification. *Applied Sciences* **10.** 8007.

Garwood NC. **1983**. Seed Germination in a Seasonal Tropical Forest in Panama: A Community Study. *Ecological Monographs* **53**: 159–181.

Gilbert GS, Harms KE, Hamill DN, Hubbell SP. **2001**. Effects of seedling size, El Niño drought, seedling density, and distance to nearest conspecific adult on 6-year survival of *Ocotea whitei* seedlings in Panamá. *Oecologia* **127**: 509–516.

Gómez-Aparicio L, Zamora R, Castro J, Hódar JA. **2008**. Facilitation of tree saplings by nurse plants: Microhabitat amelioration or protection against herbivores? *Journal of Vegetation Science* **19**: 161–172.

Grubb PJ. **1977**. The maintenance of species-richness in plant communities: the importance of the regeneration niche. *Biological Reviews* **52**: 107–145.

Hacket-Pain AJ, Ascoli D, Vacchiano G, Biondi F, Cavin L, Conedera M, Drobyshev I, Liñán ID, Friend AD, Grabner M, *et al.* 2018. Climatically controlled reproduction drives interannual growth variability in a temperate tree species. *Ecology Letters* **21**: 1833–1844.

Hanbury-Brown AR, Ward RE, Kueppers LM. 2022. Forest regeneration within Earth system models: current process representations and ways forward. *New Phytologist*, in press.

Harms KE, Condit R, Hubbell SP, Foster RB. **2001**. Habitat associations of trees and shrubs in a 50-ha neotropical forest plot. *Journal of Ecology* **89**: 947–959.

Haszpra T, Herein M, Bódai T. **2020**. Investigating ENSO and its teleconnections under climate change in an ensemble view – a new perspective. *Earth System Dynamics* **11**: 267–280.

Holm JA, Shugart HH, Van Bloem SJ, Larocque GR. 2012. Gap model development, validation, and application to succession of secondary subtropical dry forests of Puerto Rico. *Ecological Modelling* **233**: 70–82.

Hubbell SP, Foster RB, O'Brien ST, Harms KE, Condit R, Wechsler B, Wright SJ, Loo De Lao S. **1999**. Light-Gap Disturbances , Recruitment Limitation , and Tree Diversity in a Neotropical Forest. *Science* **283**: 554–558.

Jabot F, Etienne RS, Chave J. **2008**. Reconciling neutral community models and environmental filtering: theory and an empirical test. *Oikos* **117**: 1308–1320.

Johnson DJ, Condit R, Hubbell SP, Comita LS. **2017**. Abiotic niche partitioning and negative density dependence drive tree seedling survival in a tropical forest. *Proceedings of the Royal Society B: Biological Sciences* **284**: 20172210.

Johnstone JF, Chapin FS. 2006. Effects of Soil Burn Severity on Post-Fire Tree Recruitment in Boreal Forest. *Ecosystems* **9**: 14–31.

Johnstone JF, Allen CD, Franklin JF, Frelich LE, Harvey BJ, Higuera PE, Mack MC, Meentemeyer RK, Metz MR, Perry GL, *et al.* 2016. Changing disturbance regimes, ecological memory, and forest resilience. *Frontiers in Ecology and the Environment* **14**: 369–378.

Journé V, Barnagaud J, Bernard C, Crochet P, Morin X. **2020**. Correlative climatic niche models predict real and virtual species distributions equally well. *Ecology* **101**: e02912.

Kitajima K. **1994**. Relative importance of photosynthetic traits and allocation patterns as correlates of seedling shade tolerance of 13 tropical trees. *Oecologia* **98**: 419–428.

Kobe RK. **1999**. Light Gradient Partitioning among Tropical Tree Species through Differential Seedling Mortality and Growth. *Ecology* **80**: 187–201.

Kohyama TS, Kohyama TI, Sheil D. **2018**. Definition and estimation of vital rates from repeated censuses: Choices, comparisons and bias corrections focusing on trees. *Methods in Ecology and Evolution* **9**: 809–821.

Kueppers LM, Conlisk E, Castanha C, Moyes AB, Germino MJ, de Valpine P, Torn MS, Mitton JB. **2017**. Warming and provenance limit tree recruitment across and beyond the elevation range of subalpine forest. *Global Change Biology* **23**: 2383–2395.

Larocque GR, Archambault L, Delisle C. 2006. Modelling forest succession in two southeastern Canadian mixedwood ecosystem types using the ZELIG model. *Ecological Modelling* **199**: 350–362

Lebrija-Trejos E, Pérez-GarcíA EA, Meave JA, Bongers F, Poorter L. **2010**. Functional traits and environmental filtering drive community assembly in a species-rich tropical system. *Ecology* **91**: 386–398.

Lischke H, Löffler TJ. 2006. Intra-specific density dependence is required to maintain species diversity in spatio-temporal forest simulations with reproduction. *Ecological Modelling* **198**: 341–361

Lischke H, Zimmermann NE, Bolliger J, Rickebusch S, Löffler TJ. **2006**. TreeMig: A forest-landscape model for simulating spatio-temporal patterns from stand to landscape scale. *Ecological Modelling* **199**: 409–420.

Markl JS, Schleuning M, Forget PM, Jordano P, Lambert JE, Traveset A, Wright SJ, Böhning-Gaese K. **2012**. Meta-Analysis of the Effects of Human Disturbance on Seed Dispersal by Animals. *Conservation Biology* **26**: 1072–1081.

Martínez Cano I, Shevliakova E, Malyshev S, Wright SJ, Detto M, Pacala SW, Muller-Landau HC. **2020**. Allometric constraints and competition enable the simulation of size structure and carbon fluxes in a dynamic vegetation model of tropical forests (LM3PPA-TV). *Global Change Biology* **26**: 4478–4494.

Martínez-Vilalta J, Lloret F. **2016**. Drought-induced vegetation shifts in terrestrial ecosystems: The key role of regeneration dynamics. *Global and Planetary Change* **144**: 94–108.

McDowell NG, Allen CD, Anderson-Teixeira K, Aukema BH, Bond-Lamberty B, Chini L, Clark JS, Dietze M, Grossiord C, Hanbury-Brown A, *et al.* 2020. Pervasive shifts in forest dynamics in a changing world. *Science* **368**: eaaz9463–eaaz9463.

Medvigy D, Wofsy SC, Munger JW, Hollinger DY, Moorcroft PR. **2009**. Mechanistic scaling of ecosystem function and dynamics in space and time: Ecosystem Demography model version 2. *Journal of Geophysical Research: Biogeosciences* **114**: 1–21.

Minor DM, Kobe RK. **2019**. Fruit production is influenced by tree size and size-asymmetric crowding in a wet tropical forest. *Ecology and Evolution* **9**: 1458–1472.

Mitchard ETA. **2018**. The tropical forest carbon cycle and climate change. *Nature* **559**: 527–534.

Mladenoff DJ. **2004**. LANDIS and forest landscape models. *Modelling disturbance and succession in forest landscapes using LANDIS* **180**: 7–19.

Mok H-F, Arndt SK, Nitschke CR. **2012**. Modelling the potential impact of climate variability and change on species regeneration potential in the temperate forests of South-Eastern Australia. *Global Change Biology* **18**: 1053–1072.

Moorcroft PR, Hurtt GC, Pacala SW. **2001**. A method for scaling vegetation dynamics: The ecosystem demography model (ED). *Ecological Monographs* **71**: 557–586.

Notman E, Gorchov DL. **2001**. Variation in Post-dispersal Seed Predation in Mature Peruvian Lowland Tropical Forest and Fallow Agricultural Sites. *Biotropica* **33**: 621–636.

O'Brien MJ, Peréz-Aviles D, Powers JS. **2018**. Resilience of seed production to a severe El Niño-induced drought across functional groups and dispersal types. *Global Change Biology* **24**: 5270–5280.

Obroucheva N, Sinkevich I, Lityagina S. 2016. Physiological aspects of seed recalcitrance: A case study on the tree *Aesculus hippocastanum*. *Tree Physiology* **36**: 1127–1150.

d'Oliveira MVN, Ribas LA. **2011**. Forest regeneration in artificial gaps twelve years after canopy opening in Acre State Western Amazon. *Forest Ecology and Management* **261**: 1722–1731.

Paton S. **2019**. Barro Colorado Island, Lutz catchment, Soil moisture, manual. doi:https://doi.org/10.25573/data.10042517.v3. [accessed 16 February 2022].

Pearson TRH, Burslem DFRP, Mullins CE, Dalling JW. **2002**. Germination ecology of neotropical pioneers: Interacting effects of environmental conditions and seed size. *Ecology* **83**: 2798–2807.

Pearson RG, Dawson TP. **2003**. Predicting the impacts of climate change on the distribution of species: are bioclimate envelope models useful? *Global Ecology and Biogeography* **12**: 361–371.

Poorter L. **1999**. Growth responses of 15 rain-forest tree species to a light gradient: The relative importance of morphological and physiological traits. *Functional Ecology* **13**: 396–410.

Poorter L. **2007**. Are Species Adapted to Their Regeneration Niche, Adult Niche, or Both? *The American Naturalist* **169**: 433–442.

Poulter B, Ciais P, Hodson E, Lischke H, Maignan F, Plummer S, Zimmermann NE. **2011**. Plant functional type mapping for earth system models. *Geoscientific Model Development* **4**: 993–1010.

Powell TL, Koven CD, Johnson DJ, Faybishenko B, Fisher RA, Knox RG, McDowell NG, Condit R, Hubbell SP, Wright SJ, *et al.* 2018. Variation in hydroclimate sustains tropical forest biomass and promotes functional diversity. *New Phytologist* **219**: 932–946.

Powell T, Kueppers L, Paton S. **2017**. Seven years (2008-2014) of meteorological observations plus a synthetic El Nino drought for BCI Panama. doi: 10.15486/ngt/1414275. [accessed 16 February 2022].

Price DT, Zimmermann NE, Van Der Meer PJ, Lexer MJ, Leadley P, Jorritsma ITMM, Schaber J, Clark DF, Lasch P, Mcnulty S, *et al.* 2001. Regeneration in gap models: Priority issues for studying forest responses to climate change. *Climatic Change* **51**: 475–508.

R Core Team. **2020**. R: A Language and Environment for Statistical Computing (version 3.6.3). *R Foundation for Statistical Computing, Vienna, Austria*.

Rüger N, Huth A, Hubbell SP, Condit R. **2009**. Response of recruitment to light availability across a tropical lowland rain forest community. *Journal of Ecology* **97**: 1–3.

Running, S., Mu, Q., & Zhao, M. 2015. MOD17A3H MODIS/terra net primary production yearly L4 global 500m SIN grid V006. NASA EOSDIS Land Processes DAAC. https://doi.org/10.5067/MODIS/MOD17A3H.006 [accessed 16 February 2022].

Ruiz Talonia L, Reid N, Gross CL, Whalley RDB. **2017**. Germination ecology of six species of *Eucalyptus* in shrink–swell vertosols: moisture, seed depth and seed size limit seedling emergence. *Australian Journal of Botany* **65**: 22–22.

Sansevero JBB, Garbin ML, Sánchez-Tapia A, Valladares F, Scarano FR. **2020**. Fire drives abandoned pastures to a savanna-like state in the Brazilian Atlantic Forest. *Perspectives in Ecology and Conservation* **18**: 31–36.

Sato H. **2009**. Simulation of the vegetation structure and function in a Malaysian tropical rain forest using the individual-based dynamic vegetation model SEIB-DGVM. *Forest Ecology and Management* **257**: 2277–2286.

Sato H, Itoh A, Kohyama T. **2007**. SEIB-DGVM: A new Dynamic Global Vegetation Model using a spatially explicit individual-based approach. *Ecological Modelling* **200**: 279–307.

Seidl R, Thom D, Kautz M, Martin-Benito D, Peltoniemi M, Vacchiano G, Wild J, Ascoli D, Petr M, Honkaniemi J, *et al.* 2017. Forest disturbances under climate change. *Nature Climate Change* **7**: 395–402.

Serra-Diaz JM, Maxwell C, Lucash MS, Scheller RM, Laflower DM, Miller AD, Tepley AJ, Epstein HE, Anderson-Teixeira KJ, Thompson JR. **2018**. Disequilibrium of fire-prone forests sets the stage for a rapid decline in conifer dominance during the 21stcentury. *Scientific Reports* **8**: 1–12.

Scheller RM, Domingo JB, Sturtevant BR, Williams JS, Rudy A, Gustafson EJ, Mladenoff DJ. **2007**. Design, development, and application of LANDIS-II, a spatial landscape simulation model with flexible temporal and spatial resolution. *Ecological Modelling* **201**: 409–419.

Slik JWF. **2004**. El Niño droughts and their effects on tree species composition and diversity in tropical rain forests. *Oecologia* **141**: 114–120.

Smith B, Prentice IC, Sykes MT. **2001**. Representation of vegetation dynamics in modelling of European ecosystems: comparison of two contrasting approaches within European climate space. *Global Ecology and Biogeography* **10**: 621–637.

Spear ER, Broders KD. **2021**. Host-generalist fungal pathogens of seedlings may maintain forest diversity via host-specific impacts and differential susceptibility among tree species. *New Phytologist* **231**: 460–474.

Spear ER, Coley PD, Kursar TA. **2015**. Do pathogens limit the distributions of tropical trees across a rainfall gradient? *Journal of Ecology* **103**: 165–174.

Stevens-Rumann CS, Kemp KB, Higuera PE, Harvey BJ, Rother MT, Donato DC, Morgan P, Veblen TT. **2018**. Evidence for declining forest resilience to wildfires under climate change. *Ecology Letters* **21**: 243–252.

Tepley AJ, Thompson JR, Epstein HE, Anderson-Teixeira KJ. **2017**. Vulnerability to forest loss through altered postfire recovery dynamics in a warming climate in the Klamath Mountains. *Global Change Biology* **23**: 4117–4132.

Turner MG. **2010**. Disturbance and landscape dynamics in a changing world. *Ecology* **91**: 2833–2849.

Vacchiano G, Ascoli D, Berzaghi F, Lucas-Borja ME, Caignard T, Collalti A, Mairota P, Palaghianu C, Reyer CPO, Sanders TGM, *et al.* 2018. Reproducing reproduction: How to simulate mast seeding in forest models. *Ecological Modelling* **376**: 40–53.

Valdez JW, Hartig F, Fennel S, Poschlod P. **2019**. The recruitment niche predicts plant community assembly across a hydrological gradient along plowed and undisturbed transects in a former agricultural wetland. *Frontiers in Plant Science* **10**: 88–88.

Vazquez-Yanes C, Orozco-Segovia A, Medina E, Mooney HA, Vazquez-Yanes C. **1990**. Ecophysiology of Seed Germination in the Tropical Humid Forests of the World: A Review. In: Medina E, Mooney Mooney HA, Vazquez-Yanes C, eds. *Physiological ecology of plants of the wet tropics*. Dordrecht, Netherlands: Springer. https://doi.org/10.1007/978-94-009-7299-5_5.

Visser MD, Bruijning M, Wright SJ, Muller-Landau HC, Jongejans E, Comita LS, de Kroon H. **2016**. Functional traits as predictors of vital rates across the life cycle of tropical trees. *Functional Ecology* **30**: 168–180.

Walck JL, Hidayati SN, Dixon KW, Thompson K, Poschlod P. 2011. Climate change and plant regeneration from seed. *Global Change Biology* **17**: 2145–2161.

Weissflog A, Markesteijn L, Lewis OT, Comita LS, Engelbrecht BMJ. **2018**. Contrasting patterns of insect herbivory and predation pressure across a tropical rainfall gradient. *Biotropica* **50**: 302–311.

Will RE, Wilson SM, Zou CB, Hennessey TC. **2013**. Increased vapor pressure deficit due to higher temperature leads to greater transpiration and faster mortality during drought for tree seedlings common to the forest–grassland ecotone. *New Phytologist* **200**: 366–374.

Wenk EH, Abramowicz K, Westoby M, Falster DS. **2017**. Coordinated shifts in allocation among reproductive tissues across 14 coexisting plant species. *BioRxiv*. doi:10.1101/141473

Wright SJ, Bruijning M, Brassfield D, Cerezo A, Visser MD. **2015**. The Barro Colorado Island Tree Reproduction Dataset. doi:10.5479/si.data.201511251100. [accessed 16 February 2022].

Wright SJ, Calderón O. **2006**. Seasonal, El Nino and longer term changes in flower and seed production in a moist tropical forest. *Ecology Letters* **9**: 35–44.

Wright SJ, Hernandéz A, Condit R. **2007**. The bushmeat harvest alters seedling banks by favoring lianas, large seeds, and seeds dispersed by bats, birds, and wind. *Biotropica* **39**: 363–371.

Wright SJ, Kitajima K, Kraft NJB, Reich PB, Wright IJ, Bunker DE, Condit R, Dalling JW, Davies SJ, Diaz S, *et al.* 2010. Functional traits and the growth-mortality tradeoff in tropical trees. *Ecology* **91**: 3664–3674.

Wright J, Muller-Landau HC. **2005**. Annual and spatial variation in seed fall and seedling recruitment in a neotropical forest. *Ecology* **86**: 848–860.

Zhang T, Niinemets Ü, Sheffield J, Lichstein JW. **2018**. Shifts in tree functional composition amplify the response of forest biomass to climate. *Nature* **556**: 99–102.

SUPPORTING INFORMATION LEGENDS

Methods S1. Derivation of parameter values for Barro Colorado Island

Fig. S1. Observations of moisture deficit and seedling mortality

Methods S2. Assigning species to drought tolerant and drought intolerant PFTs

Note S1. The DRY-DS precipitation scenario

Fig. S2. Results from the DRY-DS precipitation scenario

Table S1. Expert classification of tree growth forms (understory, midstory, canopy) at BCI (.xlsx file)

Table S2. Species assignments to plant functional types (.xlsx file)

Figure S3. ED2 predictions of soil matric potential under BASE, WET, SYN-ENSO, and DRY-DS precipitation scenarios.

Fig. S4. ED2 predictions of PFT-specific NPP under BASE, WET, SYN-ENSO, and DRY-DS precipitation scenarios

Fig. S5. ED2 predictions of soil matric potential during a synthetic El Niño drought at Barro Colorado Island.